J Neurophysiol 103: 1543–1556, 2010.
First published January 13, 2010; doi:10.1152/jn.01121.2009.

Mitochondrial Ca^{2+} Activates a Cation Current in *Aplysia* Bag Cell Neurons

Charlene M. Hickey, Julia E. Geiger, Chris J. Groten, and Neil S. Magoski
Department of Physiology, Queen's University, Kingston, Ontario, Canada

Submitted 18 December 2009; accepted in final form 11 January 2010

Hickey CM, Geiger JE, Groten CJ, Magoski NS. Mitochondrial Ca^{2+} activates a cation current in *Aplysia* bag cell neurons. *J Neurophysiol* 103: 1543–1556, 2010. First published January 13, 2010; doi:10.1152/jn.01121.2009. Ion channels may be gated by Ca^{2+} entering from the extracellular space or released from intracellular stores—typically the endoplasmic reticulum. The present study examines how Ca^{2+} impacts ion channels in the bag cell neurons of *Aplysia californica*. These neuroendocrine cells trigger ovulation through an afterdischarge involving Ca^{2+} influx from Ca^{2+} channels and Ca^{2+} release from both the mitochondria and endoplasmic reticulum. Liberating mitochondrial Ca^{2+} with the protonophore, carbonyl cyanide-4-trifluoromethoxyphenyl-hydrazone (FCCP), depolarized bag cell neurons, whereas depleting endoplasmic reticulum Ca^{2+} with the Ca^{2+}-ATPase inhibitor, cyclopiazonic acid, did not. In a concentration-dependent manner, FCCP elicited an inward current associated with an increase in conductance and a linear current/voltage relationship that reversed near −40 mV. The reversal potential was unaffected by changing intracellular Cl^-, but left-shifted when extracellular Ca^{2+} was removed and right-shifted when intracellular K^+ was decreased. Strong buffering of intracellular Ca^{2+} decreased the current, although the response was not altered by blocking Ca^{2+}-dependent proteases. Furthermore, fura imaging demonstrated that FCCP elevated intracellular Ca^{2+} with a time course similar to the current itself. Inhibiting either the V-type H^+-ATPase or the ATP synthetase failed to produce a current, ruling out acidic Ca^{2+} stores or disruption of ATP production as mechanisms for the FCCP response. Similarly, any involvement of reactive oxygen species potentially produced by mitochondrial depolarization was mitigated by the fact that dialysis with xanthine/xanthine oxidase did not evoke an inward current. However, both the FCCP-induced current and Ca^{2+} elevation were diminished by disabling the mitochondrial permeability transition pore with the alkylating agent, *N*-ethylmaleimide. The data suggest that mitochondrial Ca^{2+} gates a voltage-independent, nonselective cation current with the potential to drive the afterdischarge and contribute to reproduction. Employing Ca^{2+} from mitochondria, rather than the more common endoplasmic reticulum, represents a diversification of the mechanisms that influence neuronal activity.

INTRODUCTION

Intracellular Ca^{2+} is a fundamental signal that impacts secretion, gene expression, and ion channel function (Greer and Greenberg 2008; Levitan 1999; Neher and Sakaba 2008). Ca^{2+} enters neurons through voltage-gated Ca^{2+} channels as well as via release from intracellular stores (Friel and Chiel 2008). The best-studied store is the endoplasmic reticulum, which may be accessed by Ca^{2+} influx stimulating ryanodine receptors (Ca^{2+}-induced Ca^{2+} release), metabotropic receptors initiating inositol triphosphate synthesis, or block of the Ca^{2+}-ATPase [by cyclopiazonic acid (CPA) or thapsigargin] permitting Ca^{2+} to leak out of the organelle (Bardo et al. 2006; Seidler et al. 1989; Solovyova et al. 2002; Thastrup et al. 1990). Endoplasmic reticulum Ca^{2+} can influence neuronal activity and excitability by acting on various ion channels, including Ca^{2+}-activated K^+ and nonselective cation channels (Crawford et al. 1997; Li et al. 1999; Tatsumi and Katayama 1994) as well as ionotropic receptors and voltage-gated Ca^{2+} channels (Emptage et al. 2001; Richter et al. 2005).

The other major reservoir is the mitochondria, which maintains high Ca^{2+} because the very negative voltage across the inner membrane makes Ca^{2+} entry electrically favorable (Campanella et al. 2004). Ca^{2+} can be liberated by collapsing this voltage with protonophores such as carbonyl cyanide 4-(trifluoromethoxy) phenylhydrazone (FCCP) (Fulceri et al. 1991; Heytler and Prichard 1962). Additionally, loading mitochondria with Ca^{2+} during action potentials can lead to subsequent release of that Ca^{2+} through exchangers (Colegrove et al. 2000; Wingrove and Gunter 1986). Mitochondria have been considered Ca^{2+} buffers or sinks with a less-than-direct role in Ca^{2+} signaling (Friel and Tsien 1994). Thus, while mitochondrial Ca^{2+} uptake certainly influences synaptic transmission and plasticity (Billups and Forsythe 2002; Tang and Zucker 1997), there is little evidence of mitochondrial Ca^{2+} itself accessing membrane channels and regulating excitability.

The bag cell neurons control reproduction in the marine mollusk, *Aplysia californica* (Kupfermann 1967; Pinsker and Dudek 1977). Stimulation of these neurons initiates a prolonged burst, referred to as the afterdischarge, which culminates in the neurohemal secretion of peptide hormones to trigger egg-laying behavior (Conn and Kaczmarek 1989). We have previously reported that the bag cell neurons present a unique form of Ca^{2+}-induced Ca^{2+} release (Geiger and Magoski 2008). This response is partially attenuated by depleting endoplasmic reticulum Ca^{2+} with CPA or blocked altogether by prior pharmacological treatments causing either mitochondrial depolarization (with FCCP) or inhibition of mitochondrial Ca^{2+} exchange. It appears that subsequent to voltage-gated Ca^{2+} entry, the mitochondria expel their Ca^{2+} to elicit further Ca^{2+} release from the endoplasmic reticulum. The present study examines the biophysical consequence of liberating Ca^{2+} from either the mitochondria (with FCCP) or the endoplasmic reticulum (with CPA) in bag cell neurons. Our rather surprising finding is that Ca^{2+} from the mitochondria, rather than the endoplasmic reticulum, causes marked depolarization by opening a cation channel. Not only do these results have implications for the afterdischarge and *Aplysia* reproduction, but broaden the general function of the mitochondria from a somewhat passive store to one capable of actively regulating membrane conductances.

METHODS

Animals and cell culture

Primary cultures of isolated bag cell neurons were attained from adult *A. californica*, weighing 150–500 g. Animals were purchased

Address for reprint requests and other correspondence: N. S. Magoski, Queen's University, Department of Physiology, 4th Floor, Botterell Hall, 18 Stuart Str., Kingston, ON K7L 3N6, Canada (E-mail: magoski@queensu.ca).

from Marinus (Long Beach, CA) or Santa Barbara Marine Biologicals (Santa Barbara, CA) and housed in an ~300 l aquarium containing continuously circulating, aerated artificial seawater (Instant Ocean; Aquarium Systems; Mentor, OH) at 14–16° on 12/12-h light/dark cycle and fed Romaine lettuce 5 times per week. Following anesthesia by injection of isotonic $MgCl_2$ (~50% of body weight), the abdominal ganglion was removed and treated for 18 h with neutral protease (13.33 mg/ml; 165859; Roche Diagnostics, Indianapolis, IN) dissolved in tissue culture artificial seawater [tcASW; containing, in mM, 460 NaCl, 10.4 KCl, 11 $CaCl_2$, 55 $MgCl_2$, 10 4-(2-hydroxyethyl)-1-piperazineethanesulfonic acid (HEPES), 1 mg/ml glucose, 100 U/ml penicillin, and 0.1 mg/ml streptomycin, pH 7.8 with NaOH]. The ganglion was then transferred to fresh tcASW, and the two bag cell neuron clusters dissected from the surrounding connective tissue. Using a fire-polished Pasteur pipette and gentle trituration, neurons were dispersed in tcASW onto 35 × 10 mm polystyrene tissue culture dishes (430165; Corning, Corning, NY, or 353001; Falcon Becton-Dickinson, Franklin Lakes, NJ). Cultures were maintained in either tcASW or, on occasion, simple culture medium [SCM; composition as per tcASW plus minimum essential medium (MEM) vitamins (0.5×; 11120052; Gibco/Invitrogen; Grand Island, NY), MEM nonessential amino acids (0.2×; 11400050; Gibco/Invitrogen), and MEM essential amino acids without L-glutamine (0.2×; 1130051; Gibco/Invitrogen)] for 1–3 days in a 14°C incubator. Experiments were carried out at 22°C. Salts were obtained from Fisher Scientific (Ottawa, ON, Canada), ICN (Irvine, CA), or Sigma-Aldrich (St. Louis, MO).

Whole cell, voltage-clamp recordings

Voltage-clamp recordings were made using an EPC-8 amplifier (HEKA Electronics; Mahone Bay, NS, Canada) and the tight-seal, whole cell method. Microelectrodes were pulled from 1.5 mm internal diameter, borosilicate glass capillaries (TW150F-4; World Precision Instruments, Sarasota, FL) and had a resistance of 1–3 MΩ when filled with intracellular saline. Pipette junction potentials were nulled immediately before seal formation. Pipette and neuronal capacitive currents were canceled and the series resistance (3–5 MΩ) was compensated to 70–80% and monitored throughout the experiment. Cell capacitance was derived from the EPC-8 whole cell capacitance compensation. Current was filtered at 1 kHz by the EPC-8 Bessel filter and sampled at 2 kHz using an IBM-compatible personal computer, a Digidata 1300 A/D converter (Axon Instruments/Molecular Devices; Sunnyvale, CA) and the Clampex acquisition program of pCLAMP 8.1 (Axon Instruments). Clampex was also used to control the membrane potential. Recordings were done in normal ASW (nASW; composition as per tcASW but with glucose and antibiotics omitted) or Ca^{2+}-free ASW [composition as per tcASW but with added 0.5 mM ethylene glycol bis(aminoethyl ether) tetraacetic acid (EGTA) as well as omitting glucose, antibiotics, and Ca^{2+}]. Usually, microelectrodes were filled with regular intracellular saline [composition in mM: 500 K-aspartate, 70 KCl, 1.25 $MgCl_2$, 10 HEPES, 11 glucose, 10 glutathione, 5 ATP (grade 2, disodium salt; Sigma), and 0.1 GTP (type 3, disodium salt; Sigma); pH 7.3 with KOH; free Ca^{2+} concentration almost always set to 300 nM, but in a few instances set to 1 μM]. In some experiments, intracellular Ca^{2+} was buffered using a high-EGTA intracellular saline with 20 mM EGTA, 5 mM $MgCl_2$, and a free Ca^{2+} concentration set at 35 nM. Ca^{2+} concentrations were calculated using WebMaxC (http://www.stanford.edu/~cpatton/webmaxcS.htm). Both intracellular salines had a calculated junction potential of 15 mV versus ASW, which was compensated by off-line subtraction. For ion substitution, a low K^+ intracellular saline (composition as per regular saline but with the K-aspartate replaced with *N*-methyl-D-glucamine and aspartic acid; junction potential of 9 mV vs. nASW) and a high Cl^- internal (composition as per regular saline but with the K-aspartate replaced with KCl) were used.

Current-clamp recording

Current-clamp recordings were made using either the EPC-8 and the whole cell current-clamp method or an Axoclamp 2B amplifier (Axon Instruments/Molecular Devices) and the sharp-electrode, bridge-balanced method. Microelectrode and intracellular solution for whole cell, current-clamp were as per whole cell, voltage-clamp. Microelectrodes for sharp-electrode current-clamp were pulled from 1.2 mm internal diameter, borosilicate glass capillaries (IB120F-4; World Precision Instruments) and had a resistance of 7–12 MΩ when filled with 2 M K-acetate (supplemented with 100 mM KCl and 10 mM HEPES; pH = 7.3 with KOH). Voltage signals were filtered at 3 kHz and sampled at 2 kHz. Current was delivered either from the amplifier, Clampex, or a S88 stimulator (Grass; Warwick, MA).

Ca^{2+} imaging

The Ca^{2+}-sensitive dye, fura-PE3 (K^+ salt; 0110; Teflabs, Austin, TX) (Vorndran et al. 1995), was injected via sharp-electrode using a PMI-100 pressure microinjector (Dagan; Minneapolis, MN), while monitoring membrane potential with the Axoclamp. Microelectrodes (as per sharp electrode, current clamp) had a resistance of 15–30 MΩ when tip-filled with 10 mM fura-PE3 and backfilled with 3 M KCl. Injections required 3–10 200- to 300-ms pulses at 50–100 kPa to fill neurons with dye—estimated to be 50–100 μM. Neurons used for imaging showed resting potentials of −50 to −60 mV and displayed action potentials that overshot 0 mV (evoked by 0.5- to 1-nA pulses from the amplifier). After dye injection, neurons were allowed to equilibrate for ≥1 h. Imaging was performed using a Nikon TS100-F inverted microscope (Nikon; Mississauga, ON, Canada) equipped with Nikon Plan Fluor ×10 [numerical aperture (NA) = 0.5], ×20 (NA = 0.5), or ×40 (NA = 0.6) objectives. The light source was a 75 W Xenon arc lamp and a multi-wavelength DeltaRAM V monochromatic illuminator (Photon Technology International; London, ON, Canada) coupled to the microscope with a liquid-light guide. Excitation wavelengths were 340 and 380 nm. Between acquisitions, the excitation illumination was blocked by a shutter, which along with the excitation wavelength, was controlled by an IBM-compatible personal computer, a Photon Technology International computer interface, and ImageMaster Pro software (version 1.49; Photon Technology International). The emitted light passed through a 510/40-nm barrier filter prior to being detected by a Photon Technology International IC200 intensified charge coupled device camera. The camera intensifier voltage was set based on the initial fluorescence intensity of the cells and maintained constant thereafter. The camera black level was set prior to an experiment such that at a gain of 1 and with no light going into the camera there was a 50:50 distribution of blue and black pixels on the display. Fluorescence intensities were sampled at 60-s intervals using regions of interests defined over the somata prior to the start of the experiment and averaged 8 frames per acquisition. The focal plane was set to approximately the middle of the neuron. The ratio of emission following 340- and 380-nm excitation (340/380) was taken to reflect free intracellular Ca^{2+} and saved for subsequent analysis. Black level determination, image acquisition, frame averaging, emitted light sampling, and ratio calculations were carried out using ImageMaster Pro.

Reagents and drug application

Solution exchanges were accomplished by manual perfusion using a calibrated transfer pipette to first replace the bath (tissue culture dish) solution. Drugs were applied as a small volume (<10 μl) of concentrated stock solution mixed with a larger volume of saline (~100 μl) that was initially removed from the bath then pipetted back into the bath. Care was taken to add drugs near the side of the dish and as far away as possible from the neurons. Bafilomycin A (B1793; Sigma-Aldrich), calpeptin (03–34–0051; Calbiochem, San Diego,

CA), carbonyl cyanide 4-(trifluoromethoxy) phenylhydrazone (FCCP; 21857; Sigma-Aldrich), cyclopiazonic acid (CPA; C1530; Sigma-Aldrich or 239805; Calbiochem), and oligomycin A (75351; Sigma-Aldrich) all required dimethyl sulfoxide (DMSO; BP231; Fisher) as a vehicle. The maximal final concentration of DMSO was 0.01 μM, which in control experiments had no effect on current, voltage, or intracellular Ca^{2+}. $NiCl_2$ (N6136; Sigma-Aldrich), 1-[β-[3-(4-methoxyphenyl) propoxy]-4-methoxyphenethyl]-1H-imidazole hydrochloride (SKF-96365; 567310; Calbiochem), xanthine (X402, Sigma-Aldrich), and xanthine oxidase (X4500, Sigma-Aldrich) were made up in distilled water. *N*-ethylmaleimide (NEM; E3876; Sigma-Aldrich) was dissolved as a stock in 100% ethanol.

Analysis

Clampfit, a program of pClamp, was used to measure current and voltage. For most of these experiments, the analysis involved comparing the average value during a steady-state baseline of 1–5 min with the average value from regions that had reached a peak for 5–30 s or remained stable for 5–10 min after the delivery of a drug. All measurements of current were normalized to cell size by dividing by whole cell capacitance (pA/pF). The current-voltage relationships and reversal potentials were determined from a difference current generated by a −90- to 0-mV ramp given before and after FCCP. To derive the difference current, the ramp current recorded prior to the addition of FCCP was subtracted from the ramp current taken at the peak of the response induced by FCCP. Conductance was derived using Ohm's law and the current during a 200-ms step from −60 to −70 mV. The percentage change was calculated from the conductance before and after addition of FCCP.

Origin (version 7; OriginLab; Northampton, MA) was used to import and plot ImageMaster Pro files as line graphs. For intracellular Ca^{2+} experiments, analysis compared the steady-state value of the baseline 340/380 ratio with the ratio from regions that had reached a peak. Hill curve fits were also generated in Origin and provided the 50% effective concentration (the concentration that is required for 50% of maximal activation) as well as the Hill coefficient.

Summary data are presented as means ± SE. Statistics were performed using Instat (version 3.0; GraphPad Software, San Diego, CA). The Kolmogorov-Smirnov method was used to test data sets for normality. If the data were normal, Student's paired or unpaired *t*-test was used to test for differences between two means, while a standard one-way ANOVA with Dunn's multiple comparisons test were used to test for differences between multiple means. In cases where data were not normal, the Welch correction was applied to Student's paired or unpaired *t*-test when testing for differences between two means, while a nonparametric Kruskal-Wallis ANOVA with Dunn's multiple comparisons test was used to test for difference between multiple means. Data were considered significantly different if the *P* value was <0.05.

RESULTS

Bag cell neurons are depolarized by the protonophore, FCCP, but not the endoplasmic reticulum Ca^{2+}-ATPase blocker, CPA

In the process of investigating bag cell neuron Ca^{2+}-induced Ca^{2+} release, Geiger and Magoski (2008) reported that the release of mitochondrial Ca^{2+} by FCCP depolarized bag cell neurons. To investigate this quantitatively, the membrane potential of cultured bag cell neurons was recorded using sharp electrode current clamp. As expected, 20 μM FCCP ($n = 18$) caused a pronounced depolarization of ~35 mV (Fig. 1*A*, *left*). On occasion, a burst of action potentials was observed along with the depolarization. To test whether the endoplasmic reticulum had a similar effect, Ca^{2+} was released by blocking the Ca^{2+}-ATPase with 20 μM CPA. Interestingly, bag cell neurons treated with CPA exhibited no change in membrane potential ($n = 8$; Fig. 1*A*, *right*). The depolarizing effect of FCCP was significant in comparison to CPA (Fig. 1*B*).

Many of the subsequent experiments were performed using whole cell electrodes instead of sharp electrodes. In whole cell mode, an ATP-containing intracellular solution is dialyzed into the cell via the pipette, which is not the case for sharp-electrode mode. To control for this, 20 μM FCCP was delivered to cultured bag cell neurons in current clamp under whole cell configuration ($n = 8$). There was no significant difference in the average change in membrane potential produced by FCCP in whole cell versus sharp-electrode (Fig. 1*B*).

FCCP, but not CPA, causes an inward current

We next examined the result of Ca^{2+} liberation from the mitochondria or the endoplasmic reticulum on membrane current. Cultured bag cell neurons were whole cell voltage-clamped at −60 mV with regular intracellular saline (K^+-aspartate based; 300 nM free Ca^{2+}) in the pipette. The release of mitochondrial Ca^{2+} with 20 μM FCCP ($n = 10$) generated a slow, inward current of ~1 pA/pF (Fig. 2*A*, *top*). Under the same conditions, depletion of endoplasmic reticulum Ca^{2+} with 20 μM CPA ($n = 9$) failed to evoke a current of significant amplitude in comparison with FCCP (Fig. 2*A*, *bottom*) nor did DMSO ($n = 7$), the vehicle used for both drugs (Fig. 2*B*). Moreover, store-interaction or differential Ca^{2+} handling did not appear to be involved, as pretreatment with CPA ($n = 9$) failed to significantly alter the amplitude of the FCCP-induced current (Fig. 2*B*). Also we failed to observe a response to CPA when the neurons were dialyzed with an intracellular

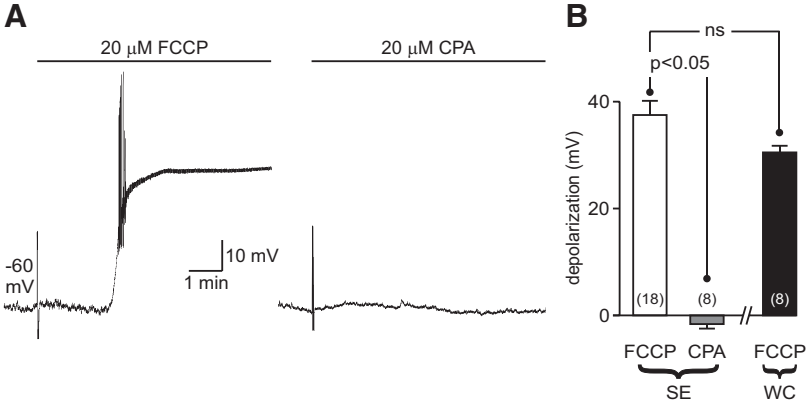

FIG. 1. Targeting the mitochondria with carbonyl cyanide-4-trifluoromethoxyphenyl-hydrazone (FCCP) but not the endoplasmic reticulum with cyclopiazonic acid (CPA) depolarizes bag cell neurons. *A*: sharp-electrode, current-clamp recordings from 2 separate bag cell neurons show that expelling Ca^{2+} from the mitochondria with 20 μM FCCP induces depolarization and spiking (*left*), but depleting endoplasmic reticulum Ca^{2+} stores with 20 μM CPA does not (*right*). *B*: summary data of the mean change in membrane potential show that the effect of FCCP readily meets the level of significance when compared with CPA (Kruskal-Wallis nonparametric ANOVA; Dunn's multiple comparisons test); however, the effect of FCCP is not significantly different when whole cell (WC), rather than sharp-electrode (SE), is employed for current-clamp recording.

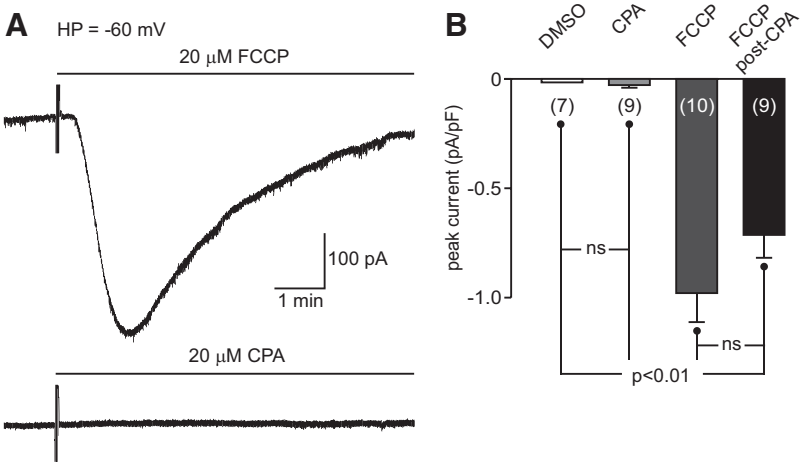

FIG. 2. FCCP, but not CPA, causes an inward current. *A*: whole cell, voltage-clamp recordings from separate neurons at −60 mV demonstrate that 20 μM FCCP (*top*) elicits an inward current but 20 μM CPA (*bottom*) does not. *B*: summary data of the mean peak current normalized to cell size (pA/pF) show that the current triggered by FCCP is significantly greater than the current produced by either CPA or the vehicle, DMSO. Furthermore, pretreatment with CPA does not significantly change the current induced by FCCP (Kruskal-Wallis nonparametric ANOVA; Dunn's multiple comparisons test).

saline containing 1 μM free Ca^{2+} (change in holding current = −0.03 ± 0.02 pA/pF $n = 4$; $P > 0.05$, one sample *t*-test).

FCCP-induced current is concentration-dependent

The 20 μM of FCCP represented a concentration our laboratory (Gardam et al. 2008; Geiger and Magoski 2008) and others (Fulceri et al. 1991; Glitsch et al. 2002; Jonas et al. 1997) have used to reliably expel mitochondrial Ca^{2+}. Because FCCP collapses mitochondrial membrane potential and releases Ca^{2+} in a concentration-dependent fashion (Heytler and Prichard 1962), we expected the FCCP-induced current would have a similar concentration dependency. To test this, FCCP was applied at 30 and 300 nM and 1, 3, and 20 μM to cultured bag cell neurons, whole cell voltage-clamped at a holding potential of −60 mV (Fig. 3*A*). The concentration-response

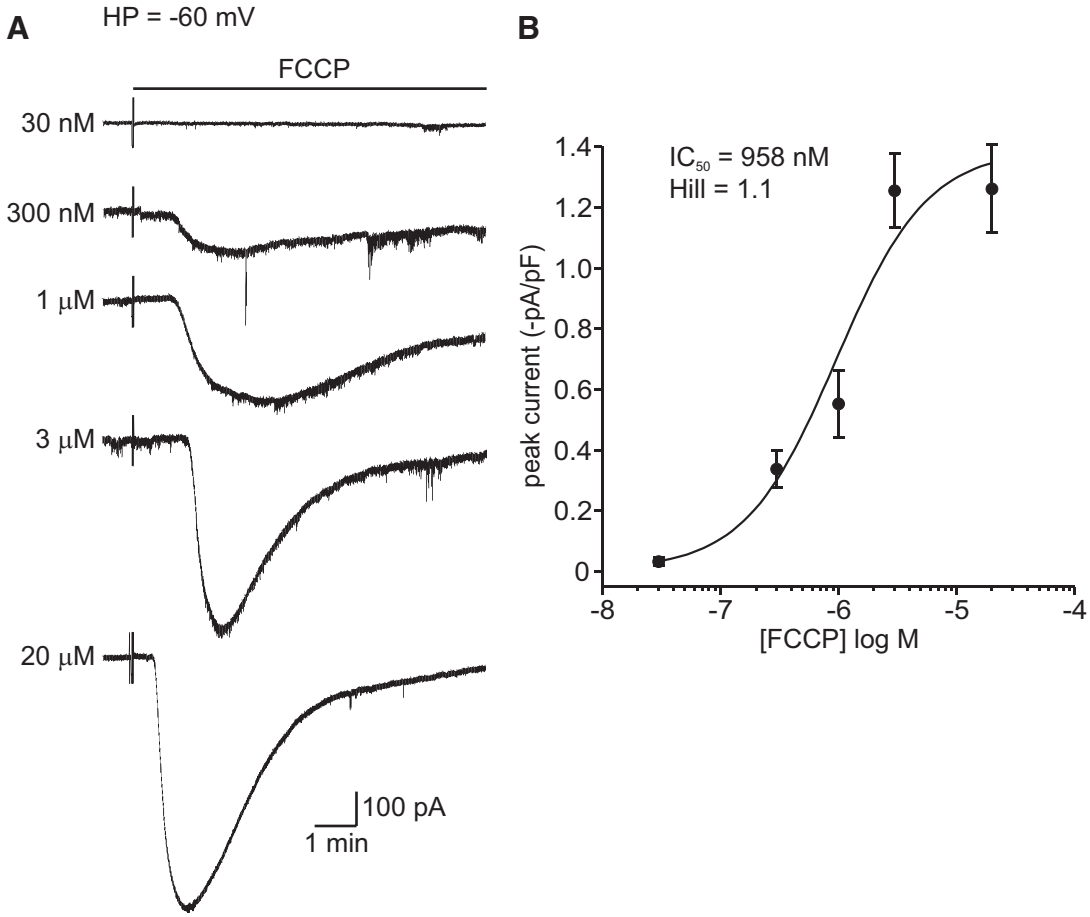

FIG. 3. The current induced by FCCP is dose-dependent. *A*: whole cell, voltage-clamp recordings from different bag cell neurons in response to 30 nM ($n = 5$), 300 nM ($n = 5$), 1 μM ($n = 5$), 3 μM ($n = 5$), and 20 μM ($n = 7$) FCCP, at a holding potential of −60 mV. *B*: the dose-response curve for FCCP reveals a half-maximal effective concentration near 1 μM, a plateau around 10 μM, and a lack of co-operativity with a Hill coefficient of 1. Only 1 neuron is exposed to a given concentration of FCCP as per the *n* value given in *A*.

curve revealed a half-maximal effective concentration of ~1 μM and a lack of cooperativity, indicated by a Hill co-efficient of 1.1 (Fig. 3*B*). Furthermore, the curve began to plateau at ~3 μM, placing 20 μM FCCP well at the top of the curve.

The time to onset of the FCCP-induced current varied from neuron to neuron as well as between concentrations. The current could appear as soon as 30 s but at times was delayed for several minutes. This is apparent in both the sample current traces displayed in Fig. 3*A* and in some of the examples provided for subsequent experiments. At every concentration, there was substantial variance in onset time with no statistical difference overall (30 nM: 2.00 ± 0.52 min, $n = 5$; 300 nM: 1.59 ± 0.63 min, $n = 5$; 1 μM: 2.82 ± 0.96 min, $n = 5$; 3 μM: 1.17 ± 0.50 min, $n = 5$; 20 μM: 2.23 ± 1.00 min, $n = 7$; $P > 0.05$, standard ANOVA). The degree of scatter was likely due to both the diffusion time of FCCP following the manual addition of the drug into the bath (see METHODS) as well as the rate at which Ca^{2+} was depleted from the mitochondria. We have observed a similar variance in onset using Ca^{2+} imaging and FCCP, both in the present study (see Figs. 6–9) and in prior work (Geiger and Magoski 2008). In addition, changes to Ca^{2+} following mitochondrial depolarization in oligodendrocytes and DRG neurons also present onset variability (Simpson and Russell 1996; Werth and Thayer 1994).

FCCP-induced current is consistent with opening of a voltage-independent cation channel

To characterize the channel responsible for the FCCP response, we examined the reversal potential and membrane conductance under control conditions and after the current induced by 20 μM FCCP had reached peak. The protocol involved delivery of a 200-ms step from −60 to −70 mV followed by a 10-s ramp from −90 to 0 mV. Changes in membrane conductance were calculated from the current during the step. The difference between the current during the ramp before and at peak was taken to be the current evoked by FCCP. The reversal potential was derived from the point where the difference current crossed the abscissa. Consistent with channel opening during the FCCP-induced current, whole cell conductance increased by over 20 times, which readily met the level of significance compared with control ($n = 9$; Fig. 4*A*). In normal extracellular saline ($n = 12$), the current-voltage relationship was largely linear and reversed around −40 mV, suggesting a voltage-independent nonselective cation channel (Colquhoun et al. 1981; Hung and Magoski 2007; Partridge et al. 1994). Some cation channels are Ca^{2+}-permeable (Chesnoy-Marchais 1985; Geiger et al. 2009; Magoski et al. 2000); when Ca^{2+} was removed from the external solution ($n = 5$), the current remained linear and the reversal shifted to approximately −47 mV, implying that Ca^{2+} passes through the channel (Fig. 4, *B* and *C*). Moreover, decreasing intracellular K^+ from 570 to 70 mM ($n = 6$), by dialyzing neurons for 30 min with low K^+ intracellular saline prior to FCCP, right-shifted the reversal to around −20 mV (Fig. 4, *B* and *C*). However, the reversal potential was not altered by raising intracellular Cl^- to 570 mM following 30-min dialysis with high Cl^- intracellular saline ($n = 4$; Fig. 4*C*). To further confirm Ca^{2+} permeability, we examined the FCCP-induced current at −60 mV only. Without extracellular Ca^{2+}, the amplitude of the FCCP-induced current was significantly diminished (Fig. 4*D*).

FCCP-induced current depends on intracellular Ca^{2+}

Release of mitochondrial Ca^{2+} into the cytosol appears to be critical for triggering the current, raising the possibility it is Ca^{2+}-activated. To test this, we dialyzed cultured bag cell neurons for 10 min with intracellular solution containing either a regular (5 mM; $n = 7$) or high (20 mM; $n = 7$) concentration of EGTA and recorded the FCCP-induced current in whole cell voltage-clamp at −60 mV. If the current was dependent on intracellular Ca^{2+} elevation, the high-EGTA should buffer the Ca^{2+} released from mitochondria and inhibit the response (Naraghi 1997). The FCCP-induced current was attenuated by nearly 2/3 with a high concentration of EGTA (Fig. 5*A*). This decrease represented a significant reduction in the amplitude of the current compared with regular internal (Fig. 5*B*). The possibility that mitochondrial Ca^{2+} increased membrane permeabilty nonspecifically by upregulating Ca^{2+}-sensitive proteases was addressed with the Ca^{2+} protease inhibitor, calpeptin (Mani et al. 2008; Tsujinaka et al. 1988). As compared with DMSO-exposed neurons ($n = 5$), pretreating neurons for 20–30 min with 100 μM calpeptin ($n = 4$) did not alter the FCCP-induced current (Fig. 5, *C* and *D*). This concentration of calpeptin has been shown to block cytosolic Ca^{2+}-activated proteases in other *Aplysia* neurons (Khoutorsky and Spira 2008; Spira et al. 2001).

Thus far, the data indicated that FCCP activates a cation current by liberating mitochondrial Ca^{2+}. Prior reports from both our laboratory and others show that FCCP as well as CPA increase intracellular Ca^{2+} (Geiger and Magoski 2008; Jonas et al. 1997; Kachoei et al. 2006; Magoski et al. 2000), yet there has been little in the way of direct comparison of either kinetics or amplitude of these responses. To examine this quantitatively, we measured intracellular Ca^{2+} using ratiometric imaging of fura PE3-injected cultured bag cell neurons. With external Ca^{2+} removed, 20 μM FCCP ($n = 19$) caused a rapid and prominent elevation in cytosolic Ca^{2+} that persisted for several min (Fig. 6*A*, *top*). Delivery of 20 μM CPA also evoked an increase in cytosolic Ca^{2+}, although this response was less than half of that observed with FCCP and typically decayed more quickly over time (Fig. 6*A*, *lower*). Overall, the mean change in Ca^{2+} caused by FCCP reached the level of significance when compared with CPA (Fig. 6*B*). We have previously shown that CPA sufficiently depletes Ca^{2+} from the endoplasmic reticulum such that it evokes store-operated Ca^{2+} influx (Kachoei et al. 2006). As an internal control, extracellular Ca^{2+} was reintroduced to those neurons that had been exposed to CPA, and in a manner typical of store-operated Ca^{2+} influx (Nilius 2003), this increased intracellular Ca^{2+} (mean peak change in 340/380: 0.08 ± 0.02; $n = 12$; Fig. 6*A*; *bottom right*).

Mechanistically different mitochondrial disruptor fails to evoke a current

The action of FCCP on the mitochondria is to collapse the H^+ gradient, which in addition to releasing Ca^{2+} also uncouples the respiratory chain. Despite our experiments supplying ATP in the whole cell pipette, it was important to control for the potential effects of FCCP on ATP synthesis. Thus we applied the mitochondrial ATPase inhibitor, oligomycin A (Fluharty and Sanadi 1963; Lardy et al. 1958), while either monitoring current or intracellular Ca^{2+}. In neurons whole cell voltage-clamped at −60 mV in nASW, 20 μM FCCP ($n = 6$)

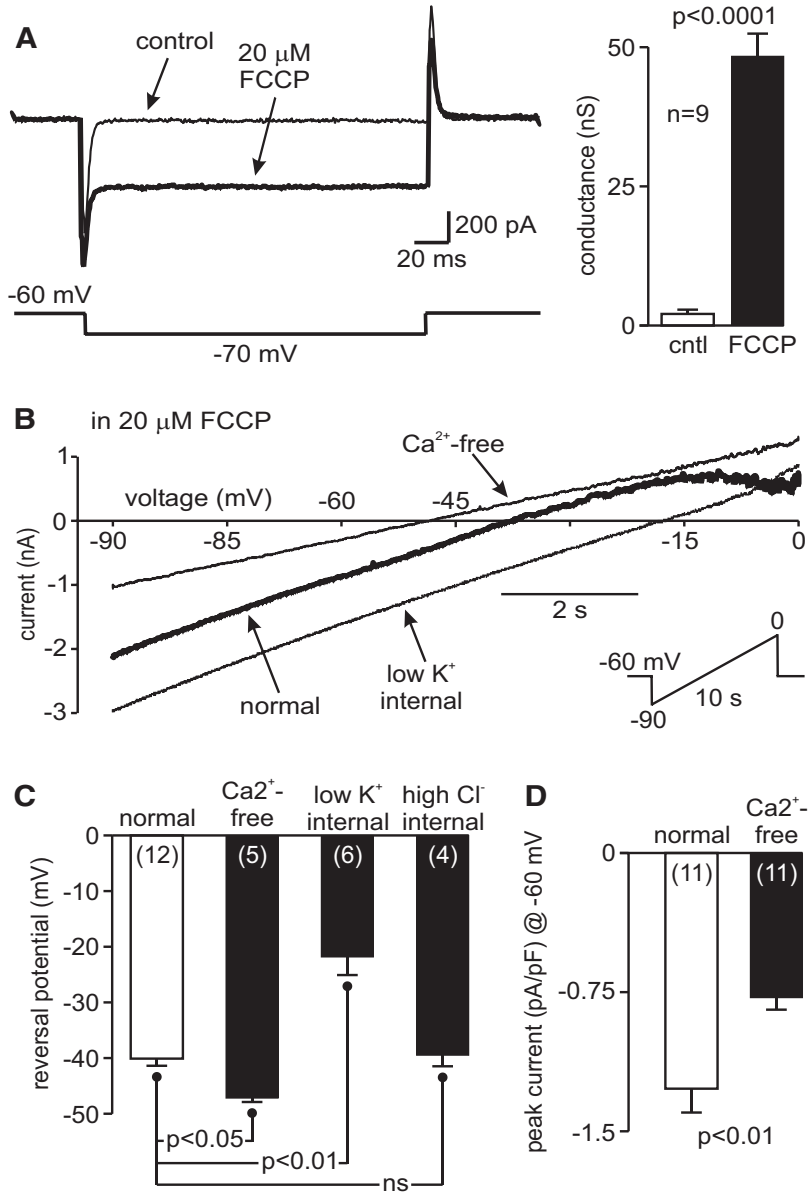

FIG. 4. The FCCP-induced current is consistent with the opening of a voltage-independent cation channel. *A, left*: whole cell, voltage-clamp recording of current during a 10-mV hyperpolarizing step from a holding potential of −60 mV before (thin line) and after (thick line) 20 μM FCCP reveals a marked elevation in conductance. Data are aligned for the purposes of comparison. *Right*: summary data show that FCCP significantly increases conductance compared with control (2-tailed paired *t*-test). *B*: subtraction current (FCCP minus control) during a ramp from −90 to 0 mV (see *inset*). In normal artificial seawater (nASW, thick line, *middle*), the FCCP-induced current is largely linear and reverses near −40 mV. In Ca^{2+}-free external (thin line, *left*), the reversal is left-shifted although the current remains linear. When intracellular K^+ is reduced by dialysis with low K^+ internal (thin line, *right*), the current reverses at a more depolarized potential of around −20 mV. A degree of inward rectification at voltages approaching 0 mV is apparent in the nASW current trace. This is observed for 1/3 to 1/2 of cases in all 3 ionic conditions (5 of 12 for nASW, 3 of 5 for Ca^{2+}-free external, and 2 of 6 for low K^+ internal). *C*: consistent with a cation channel mediating the FCCP-induced current, a lack of extracellular Ca^{2+} significantly shifts the mean reversal potential from approximately −40 to −47 mV, low intracellular K^+ significantly alters the reversal to nearly −20 mV, while high intracellular Cl^- has no significant affect (standard ANOVA; Dunn's multiple comparisons test). *D*: summary data of the mean peak current normalized to cell size show that the removal of extracellular Ca^{2+} significantly decreases the amplitude of the current evoked by FCCP (2-tailed unpaired *t*-test; Welch corrected).

consistently induced an inward current, while 5 μg/ml oligomycin A failed to evoke current ($n = 6$) or alter the FCCP-induced current ($n = 6$; Fig. 7*A*). There was no significant change in the current produced by FCCP after pretreatment with oligomycin A; however, there was a significant difference between the average amplitude of the current generated by FCCP alone and oligomycin A alone (Fig. 7*C*). This could reflect that specific timing of mitochondrial Ca^{2+} release is critical in activation of the current, or that oligomycin A liberates Ca^{2+} from another source. During imaging in Ca^{2+}-free external, FCCP evoked a robust increase in intracellular Ca^{2+} ($n = 12$), while oligomycin A caused a modest elevation, with the onset taking approximately twice as long and the peak taking about five times as long ($n = 27$; Fig. 7*B*). The average rise in Ca^{2+} observed in response to oligomycin A was significantly lower than that to FCCP (Fig. 7*D*); furthermore, when FCCP was added after oligomycin A had elevated Ca^{2+} ($n = 10$), it did not significantly affect the amplitude of the FCCP-induced Ca^{2+} increase.

Depolarization of the mitochondria has the potential to release reactive oxygen species (Galluzzi et al. 2009), which in turn could contribute to current activation. This prospect was tested by dialyzing neurons with 250 μM xanthine and 2.5 U of xanthine oxidase while recording holding current under whole cell voltage clamp at −60 mV. The effect on inward current of the reactive oxygen species generator cocktail, which readily produces superoxide (C. A. Ward, personal communication) (see also Link and Riley 1988), was a minimal change of -0.11 ± 0.11 pA/pF over the course of 20–30 min ($n = 5$; $P > 0.05$, 1-sample *t*-test).

Disruptor of acidic store H^+ transport does not induce a current

A second consideration is that as a protonophore, FCCP has the potential to release Ca^{2+} by collapsing the H^+ gradient of the acidic store as well as the mitochondria. The acidic store (vesicles, lysosomes) accumulates Ca^{2+} using H^+/Ca^{2+} ex-

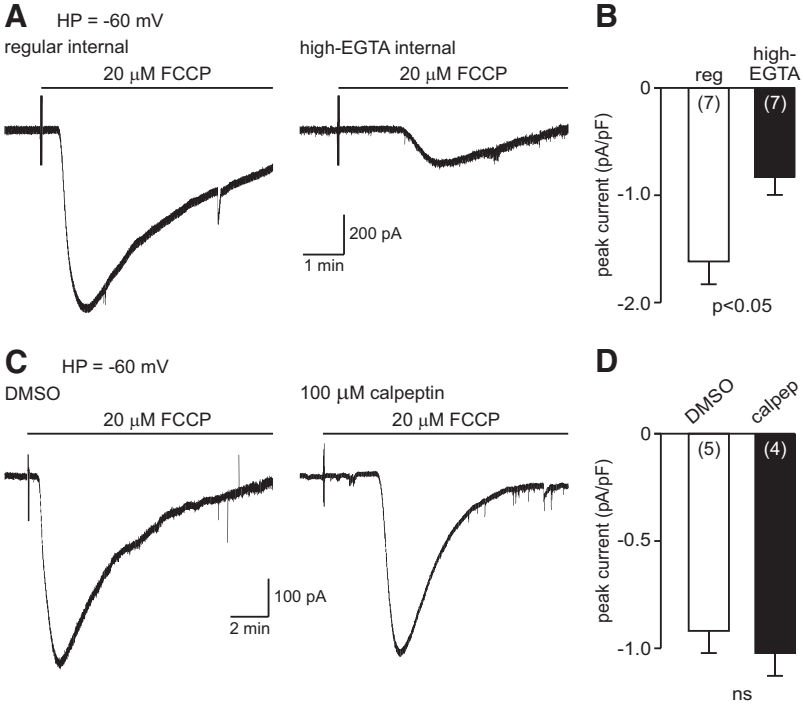

FIG. 5. Buffering intracellular Ca^{2+} decreases the amplitude of the FCCP-induced current. *A*: whole cell, voltage-clamp recordings from two different neurons at a holding potential of −60 mV show that the current produced by FCCP in the presence of regular EGTA (5 mM; *left*) is inhibited when intracellular Ca^{2+} is buffered by a high concentration of EGTA (20 mM; *right*) in the pipette. In both cases, the neurons are dialyzed for 10 min prior to the addition of FCCP. The delay in current onset with high-EGTA is not characteristic of this experimental condition and is found in both data sets. *B*: summary data show that the mean peak current density elicited by 20 μM FCCP is significantly reduced when regular internal is replaced with high-EGTA internal (2-tailed unpaired *t*-test). *C*: current traces from 2 different neurons at a holding potential of −60 mV demonstrate that the response to FCCP subsequent to DMSO (*left*) is not changed by a 20-min pretreatment with 100 μM of the protease inhibitor, calpeptin (*right*). *D*: the average peak current observed following 20 μM FCCP and normalized to cell size is not significantly impacted by calpeptin (2-tailed unpaired *t*-test).

change and a H^+ gradient maintained by a H^+-ATPase (Christensen 2002; Goncalves et al. 1999). Thus it is possible that acidic store Ca^{2+} contributes to the FCCP-induced current. However, while 20 μM FCCP elicited an inward current in cultured bag cell neurons whole cell voltage-clamped at −60 mV ($n = 6$), this was not the case for 100 nM of the V-type H^+-ATPase inhibitor, bafilomycin A (Bowman et al. 1988) ($n = 5$; Fig. 8*A*). Moreover, prior expulsion of bafilomycin A-sensitive stores did not alter the FCCP-induced current ($n = 5$; Fig. 8, *A* and *C*). The amplitude of the current produced by FCCP was significantly greater compared with bafilomycin A (Fig. 8*C*). Imaging in Ca^{2+}-free external showed 20 μM FCCP caused a marked elevation that peaked within minutes ($n = 13$), while bafilomycin A elicited a far more gradual increase that plateaued at an amplitude just 15% of FCCP (Fig. 8*B*). FCCP evoked a significantly greater peak change in 340/380 compared with bafilomycin A (Fig. 8*D*). Additionally, following prior liberation of Ca^{2+} from acidic stores, the subsequent rise in Ca^{2+} caused by FCCP was not altered ($n = 7$) (Fig. 8, *B* and *D*).

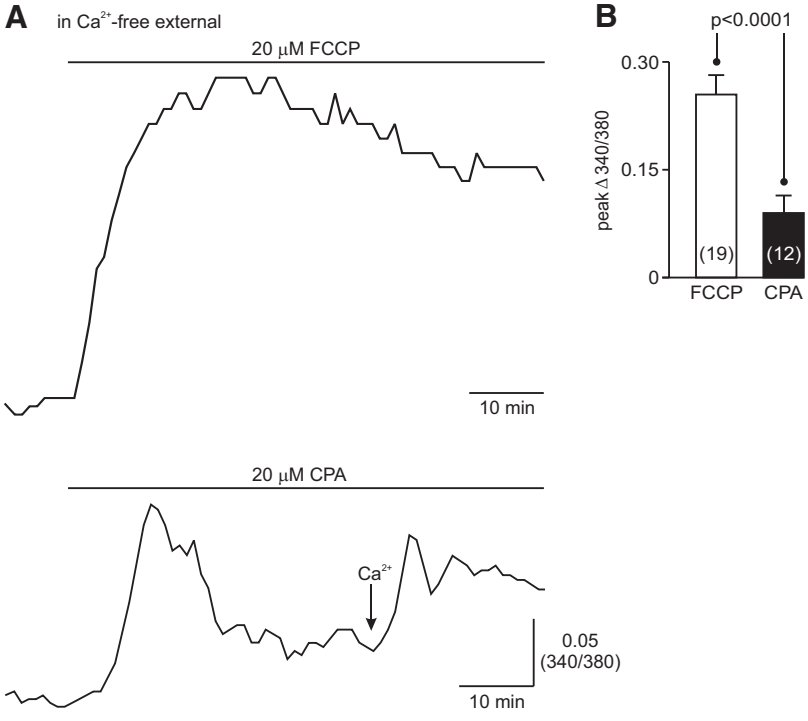

FIG. 6. Both FCCP and CPA increase intracellular Ca^{2+}. *A*: ratiometric imaging of intracellular Ca^{2+} in fura PE3-injected bag cell neurons. In Ca^{2+}-free external, 20 μM FCCP (*top*) depletes the mitochondria of Ca^{2+} and causes an elevation in cytosolic Ca^{2+} as indicated by an increase in the intensity of the 340/380 ratio. A cell exposed to 20 μM CPA (*bottom*), also shows rise in intracellular Ca^{2+}, albeit not as large as that seen with FCCP. Confirming that the endoplasmic reticulum is actually depleted by CPA, the addition of extracellular Ca^{2+} (at arrow) consistently results in a secondary rise in intracellular Ca^{2+}, i.e., store-operated influx. *B*: summary data of the mean change in 340/380 show that the effect of FCCP readily meets significance compared with CPA (2-tailed unpaired *t*-test; Welch corrected).

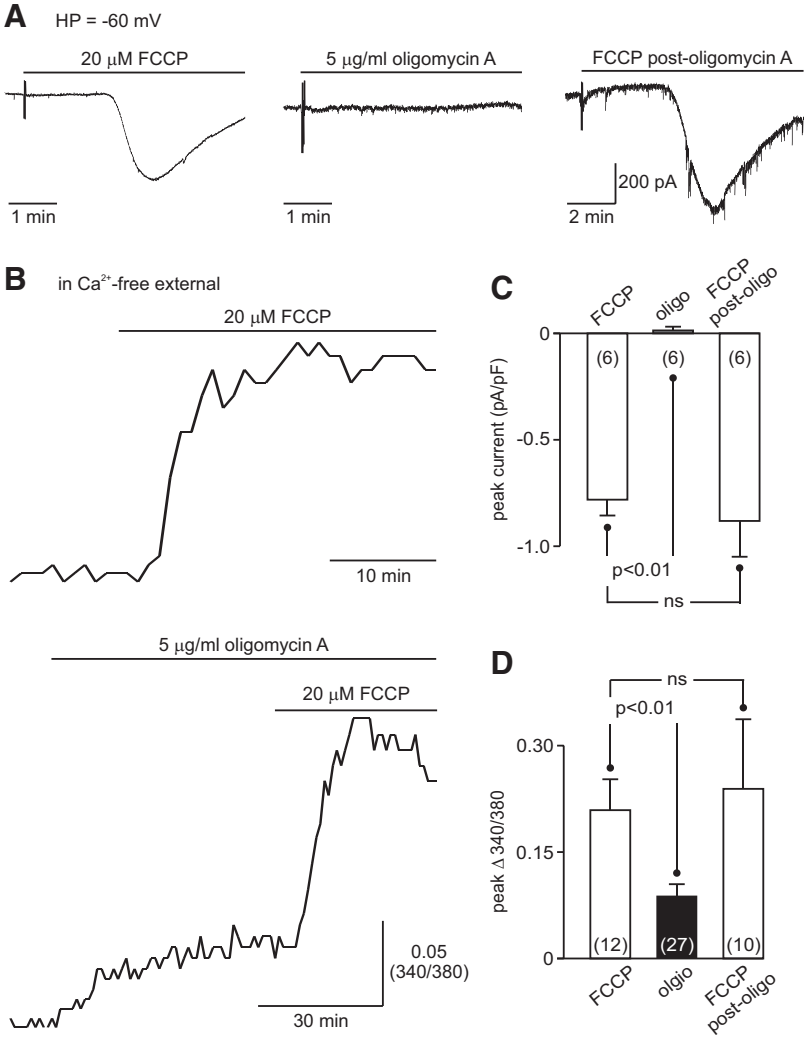

FIG. 7. Blocking the mitochondrial ATP synthetase increases intracellular Ca^{2+} but fails to produce a current. *A*: whole cell, voltage-clamp recordings from 3 separate neurons at −60 mV demonstrate that an inward current is brought about by 20 μM FCCP (*right*), but not by 5 μg/ml oligomycin A (*middle*), a blocker of the mitochondrial ATP synthetase; additionally, the FCCP-induced current is not sensitive to pretreatment with oligomycin A (*left*). *B*: intracellular Ca^{2+} is measured using ratiometric imaging in 2 cultured bag cell neurons injected with fura PE3. Without Ca^{2+} in the extracellular saline, 20 μM FCCP produces a sharp elevation in cytosolic Ca^{2+} (*top*). A slower rise in cytosolic Ca^{2+} that is about 1/3 the size of FCCP is seen in response to 5 μg/ml oligomycin A (*bottom*). Pretreatment with oligomycin A does not appear to alter the Ca^{2+} elevation evoked by FCCP. Note that the time base in the *bottom panel* is 3 times that of the *top panel*. *C*: summary data of the mean peak current normalized to cell size detail that the difference between the current generated by FCCP and oligomycin A readily reaches significance; however, no difference is found when comparing the current triggered by FCCP alone to FCCP following oligomycin A pretreatment. *D*: summary data of the mean change in 340/380 reveal that oligomycin A evokes an increase in cytosolic Ca^{2+} that is significantly less than that elicited by FCCP; as well, addition of FCCP following oligomycin A does not significantly affect the resulting Ca^{2+} increase (Kruskal-Wallis nonparametric ANOVA; Dunn's multiple comparisons test).

Alkylating agent attenuates the effect of FCCP on both current and intracellular Ca^{2+}

Two primary ways for Ca^{2+} to leave the mitochondria following loss of organelle membrane potential are through the mitochondrial Ca^{2+} uniporter or the mitochondrial permeability transition pore (Campanella et al. 2004). If the release of Ca^{2+} from the mitochondria can be prevented by blocking the uniporter or the transition pore, then the current initiated by FCCP should also be reduced. Ruthenium red has been used to block the uniporter in both Ca^{2+} imaging and electrophysiology experiments involving mitochondrial function (Kirichok et al. 2004; Matlib et al. 1998). Cultured bag cell neurons were dialyzed for 30 min with intracellular saline containing 100 μM ruthenium red before applying 20 μM FCCP. The amplitude of the current triggered by FCCP was unaffected by ruthenium red (control: -0.574 ± 0.088 pA/pF, $n = 6$ vs. ruthenium red: -0.585 ± 0.049 pA/pF, $n = 5$; $P > 0.05$, 1-tailed unpaired *t*-test).

We also explored the role of Ca^{2+} release through the mitochondrial permeability transition pore by delivering 20 μM FCCP to cultured bag cell neurons that had been pretreated for 30 min with either 100 μM NEM or ethanol (the vehicle). As an alkylating agent, NEM can inhibit the transition pore (Costantini et al. 1996; Hunter and Haworth 1979; Petronilli et al. 1994). Exposure to NEM lowered the current amplitude, but not the time course, by half (Fig. 9*A*). On average, the current was significantly reduced following treatment with NEM compared with ethanol (Fig. 9*B*). It was essential to take into account that attenuation of the current by NEM could be due to block of mitochondrial Ca^{2+} release or the plasma membrane channel itself. To verify that NEM was directly reducing Ca^{2+} release from FCCP-sensitive stores, intracellular Ca^{2+} was monitored in cultured bag cell neurons. In an absence of extracellular Ca^{2+}, the elevation in cytosolic Ca^{2+} evoked by 20 μM FCCP was considerably diminished following 30-min treatment with 100 μM NEM ($n = 10$) compared with ethanol ($n = 9$; Fig. 9*C*). The mean rise in intracellular Ca^{2+} triggered by FCCP was significantly lowered (nearly 40%) in the presence of NEM (Fig. 9*D*). As a further control for secondary effects, we examined the consequence of NEM exposure on a cation current elicited by Ca^{2+} influx (see DISCUSSION for a listing of the similarities between this current and the FCCP-evoked current). As our laboratory has characterized previously (Hung and Magoski 2007), a 5-Hz, 1-min train of 75-ms steps to +10 mV from a holding potential of −60 mV results in Ca^{2+} influx and the triggering of an inward current. Neurons in 100 μM NEM ($n = 4$) showed no difference in the size of this current versus cells in ethanol ($n = 5$; Fig. 9, *E* and *F*). In

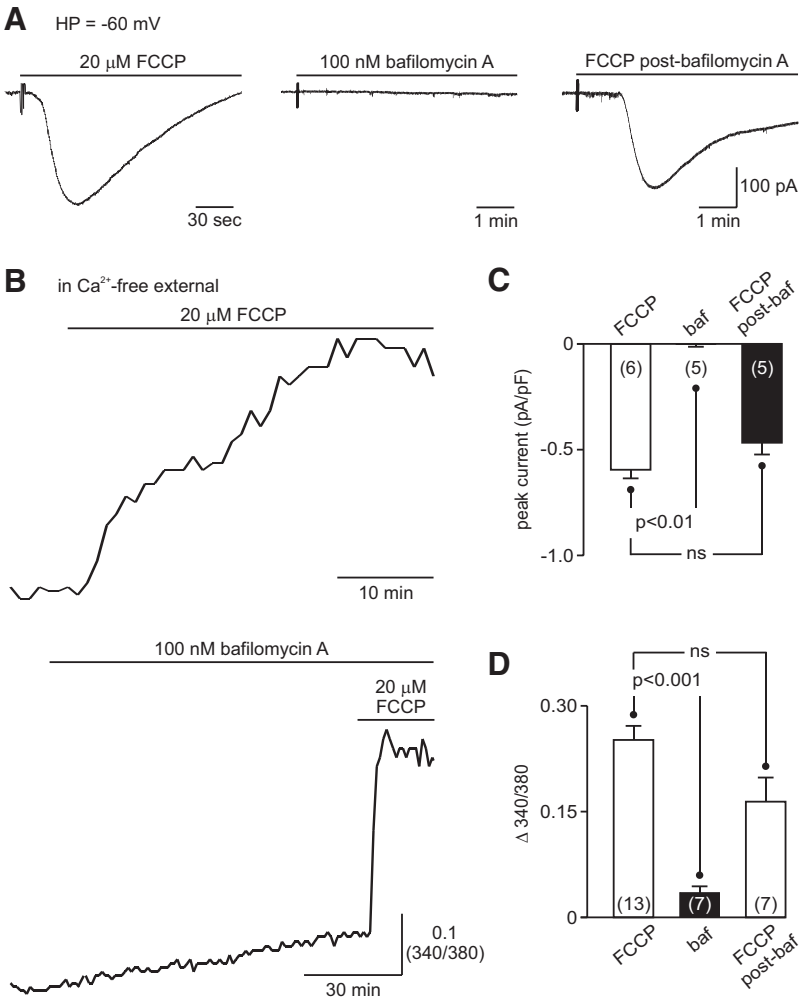

FIG. 8. Liberating acidic store Ca^{2+} does not elicit a current. *A*: whole cell, voltage-clamp recordings at −60 mV show that releasing Ca^{2+} from mitochondrial stores with 20 μM FCCP elicits an inward current (*right*), while accessing acidic stores with 100 nM bafilomycin A does not (*middle*). Furthermore, the current evoked by FCCP persists despite prior liberation of the bafilomycin-sensitive stores (*left*). Both the *middle* and *left traces* are from the same neuron, while the *right trace* is from a separate neuron. *B*: in the absence of extracellular Ca^{2+}, ratiometric imaging of 2 separate fura PE3-injected neurons demonstrates that depletion of FCCP-sensitive stores causes a relatively quick elevation in cytosolic Ca^{2+} (*top*), compared with the very slow rise seen with expelling of stores sensitive to the H^+-ATPase inhibitor, bafilomycin A (*bottom*). In addition, following bafilomycin A, FCCP causes essentially the same elevation in intracellular Ca^{2+} as control. Note that the time base in the *bottom panel* is 3 times that of the *top panel*. *C*: summary data of the mean peak current normalized to cell size indicate that FCCP produces a significantly greater current than bafilomycin A (Baf), but any change to the average FCCP-induced current following 20 min pretreatment with bafilomycin A is not significant (Kruskal-Wallis nonparametric ANOVA; Dunn's multiple comparisons test). *D*: summary data of the mean change in 340/380 indicate that the increase produced by FCCP is significantly greater compared with bafilomycin A (Kruskal-Wallis nonparametric ANOVA; Dunn's multiple comparisons test). Furthermore, while the average response elicited by FCCP with prior application of bafilomycin A appears smaller, consistent with the protonophoric action of FCCP depleting Ca^{2+} from both acidic and mitochondrial stores, it does not reach significance.

summary, NEM reduced both the FCCP-induced current and Ca^{2+} change, suggesting the current is triggered by mitochondrial Ca^{2+}.

FCCP-induced current and depolarization are not sensitive to Ni^{2+}

In addition to the evoked current, the FCCP-induced depolarization may be furthered by recruitment of voltage-sensitive channels. For example, modest depolarization can trigger a Ni^{2+}-sensitive persistent Ca^{2+} current in bag cell neurons (Tam et al. 2009). To determine if this Ca^{2+} current plays any role in the FCCP response, we first confirmed that Ni^{2+} does not block the FCCP-induced current. Cultured bag cell neurons were whole cell voltage-clamped and pretreated with 10 mM Ni^{2+} before applying 20 μM FCCP. There was no significant difference in the current in the presence ($n = 6$) or absence ($n = 6$) of Ni^{2+} (Fig. 10, *A* and *B*). A similar result was obtained using 20 μM of the store-operated channel blocker, SKF-96365 (Cabello and Schilling 1993; Kachoei et al. 2006) (control: -1.00 ± 0.24 nA/nF, $n = 5$ vs. SKF-96365: -1.23 ± 0.14 pA/pF, $n = 6$; $P > 0.05$, 1-tailed unpaired *t*-test). Next, whether Ni^{2+} had any effect on the depolarization evoked by FCCP was considered in sharp electrode current clamp. The spiking that sometimes coincided with the FCCP-induced depolarization was consistently abolished following Ni^{2+} pretreatment, which is not surprising because Ca^{2+} channels are responsible for a significant portion of the rising phase of the action potential in bag cell neurons (Acosta-Urquidi and Dudek 1981) (Fig. 10*C*). However, pretreatment with Ni^{2+} ($n = 5$) did not significantly alter the FCCP-induced depolarization ($n = 18$; Fig. 10, *C* and *D*). These observations provide evidence against the involvement of Ca^{2+} channels in the depolarization elicited by FCCP.

DISCUSSION

To the best of our knowledge, the present study is the first to indicate that mitochondrial Ca^{2+}, rather than endoplasmic reticulum Ca^{2+}, preferentially gates a membrane channel. This current produces substantial depolarization in cultured bag cell neurons, appears to be mediated by a cation conductance, and is attenuated by strong buffering of intracellular Ca^{2+} or interfering with mitochondrial Ca^{2+} release. The afterdischarge of intact bag cell neurons is associated with Ca^{2+}-induced Ca^{2+} release (Fisher et al. 1994), which we have shown to be dependent on Ca^{2+} from the mitochondria (Geiger and Magoski 2008). Thus cation channel activation by mitochondrial Ca^{2+} may further the afterdischarge and play a role in hormone secretion responsible for reproductive behavior.

Due to the very negative voltage across the mitochondrial membrane, Ca^{2+} enters from the cytosol via the Ca^{2+}

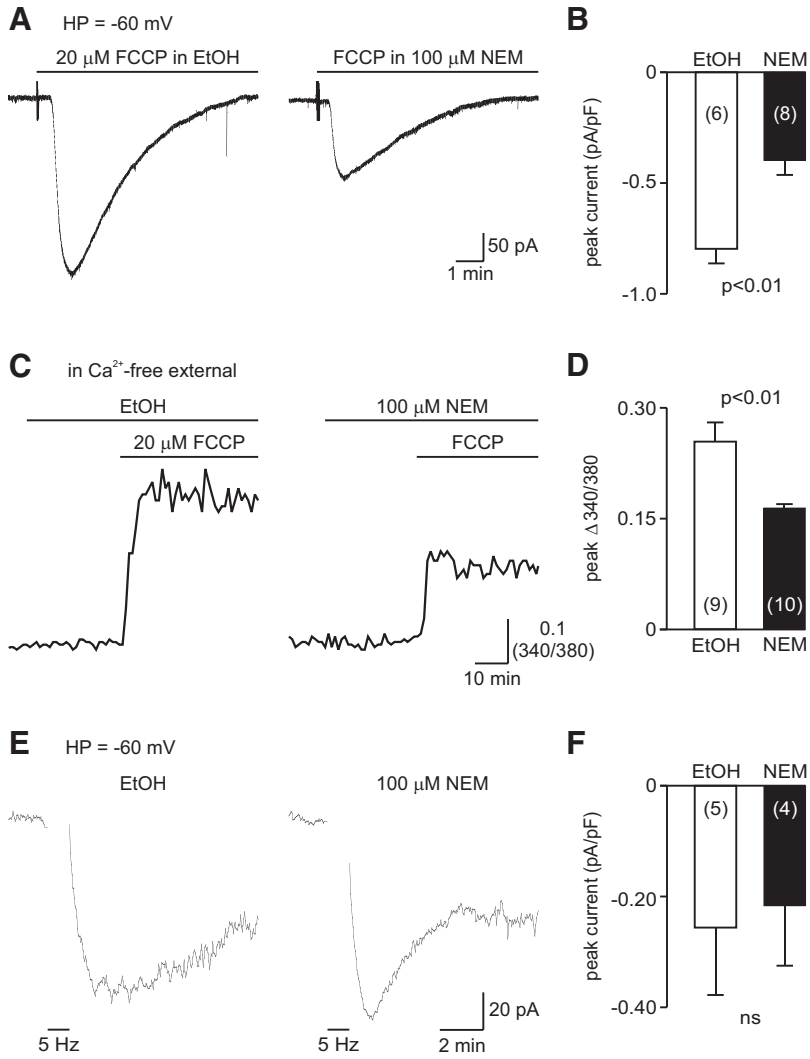

FIG. 9. An alkylating agent attenuates both the rise in intracellular Ca^{2+} and the current induced by FCCP. *A*: whole cell, voltage-clamp recordings at −60 mV, in separate neurons bathed in nASW, demonstrate a notable reduction in the amplitude of the FCCP-induced current following a 30-min pretreatment with 100 μM *N*-ethylmaleimide (NEM; *right*) but not the vehicle, ethanol (EtOH; *left*). *B*: summary data of mean peak current normalized to cell size indicate that the current evoked by 20 μM FCCP is significantly decreased subsequent to treatment with NEM versus ethanol (2-tailed unpaired *t*-test). *C*: monitoring intracellular Ca^{2+} with ratiometric imaging in Ca^{2+}-free external shows that 20 μM FCCP causes a prominent rise in cytosolic Ca^{2+} with ethanol (*left*); however, this effect is greatly diminished following a 30-min treatment with NEM (*right*). Note that application of ethanol or NEM alone does not alter intracellular Ca^{2+}. *D*: summary data show that the mean change in 340/380 evoked by FCCP is significantly less following NEM than after ethanol (2-tailed unpaired *t*-test; Welch corrected). *E*: current traces under voltage clamp at −60 mV from different neurons. Delivery (at bar) of a 5-Hz, 1-min train of 75-ms steps to +10 mV elicits an inward current. Compared with ethanol exposure (*left*), the magnitude of the train-evoked current subsequent to NEM (*right*) is similar. Differences in time-course following the peak are observed in both data sets and similar to our prior observations (see Hung and Magoski 2007). *F*: summary of average peak train-evoked current normalized to capacitance. This activity-dependent current is not significantly different when ethanol is compared with NEM (2-tailed unpaired *t*-test).

uniporter; FCCP takes the voltage to zero and causes Ca^{2+} to exit (Heytler and Prichard 1962; Moore 1971). Invertebrate examples include FCCP-induced depolarization or Ca^{2+} release from mitochondria isolated from flatworm or squid giant axon (Brinley et al. 1977; Mercer et al. 1999). Regarding Ca^{2+} handling, the uniporter is a ruthenium red-sensitive, voltage-independent ion channel in the inner membrane that could allow for Ca^{2+} efflux from depolarized mitochondria (Kirichok et al. 2004; Moore 1971). However, this channel shows extreme inward rectification near 0 mV, and efflux would be eliminated on depolarization. Hence it is not surprising that ruthenium red was ineffective at blocking the FCCP-induced current in bag cell neurons. Alternatively, Ca^{2+} could leave through the mitochondrial permeability transition pore, an inner membrane, voltage-dependent mega-channel opened by mitochondrial depolarization and blocked by NEM (Hunter and Haworth 1979). The actions of NEM on the transition pore are well characterized and reasonably specific; however, the drug is capable of altering sulfhydryl groups on a number of proteins (Costantini et al. 1996; Petronilli et al. 1994). Nevertheless, consistent with mitochondrial Ca^{2+} being the trigger, high intracellular EGTA reduces the FCCP current, while NEM lessens both the Ca^{2+} elevation and current evoked by FCCP. Furthermore NEM fails to alter the current opened by Ca^{2+} entry following a train of depolarizing stimuli (the present study) as well as the voltage-gated Ca^{2+} current itself (Hickey 2009), suggesting that akylation does not generally inhibit plasma membrane channels in bag cell neurons.

Because FCCP affects mitochondrial function, lowered ATP levels, rather than Ca^{2+} release, could influence the current. Oligomycin A blocks the mitochondrial ATP synthetase, which, like FCCP, would eliminate mitochondrial ATP production (Fluharty and Sanadi 1963; Lardy et al. 1958). It appears that glycolysis is able to provide sufficient levels of ATP in the short term despite reduced oxygen consumption in the face of mitochondrial poisoning (Land et al. 1999). The source of the oligomycin A-induced Ca^{2+} elevation in bag cell neurons may not be mitochondrial. Reduced ATP levels could result in Ca^{2+} loss from the endoplasmic reticulum or acidic stores, which depend on energy for Ca^{2+} uptake. However, our laboratory has reported that FCCP does not deplete Ca^{2+} from the endoplasmic reticulum (Geiger and Magoski 2008). Regardless of origin, Ca^{2+} liberated by oligomycin A does not evoke a current in bag cell neurons, substantiating the assertion that the FCCP-induced current is not due to changes in ATP. Additionally, we recorded the current using whole cell and ATP in the pipette.

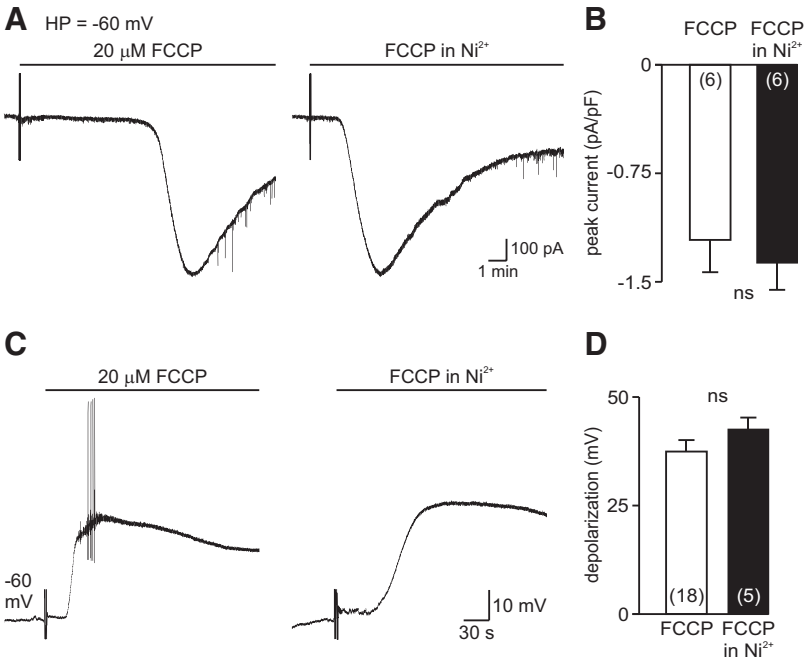

FIG. 10. Ni^{2+} does not block the FCCP-induced current or depolarization. *A*: whole cell, voltage-clamp recordings at −60 mV of separate neurons, with (*right*) and without (*left*) 5 min of 10 mM Ni^{2+} pretreatment, indicate that Ni^{2+} does not alter the amplitude of the FCCP-induced current. *B*: summary data show no significant difference in the mean peak current, normalized to cell size, elicited by 20 μM FCCP in the presence or absence of Ni^{2+} (1-tailed unpaired *t*-test). *C*: sharp-electrode current-clamp recordings in separate neurons show that the FCCP-induced depolarization is not altered by 5 min of 10 mM Ni^{2+} pretreatment. The firing of action potentials in response to FCCP is observed in 8 of the 18 neurons under control conditions (*left*); however, this response is consistently eliminated in all 5 neurons previously exposed to Ni^{2+} (*right*). *D*: summary data of the mean change in membrane potential show that the depolarization induced by FCCP is not significantly different, with or without Ni^{2+} pretreatment (2-tailed unpaired *t*-test).

FCCP theoretically increases the permeability of H^+ across all membranes, potentially allowing H^+ to contribute to resting potential (Bashford et al. 1985). However, this would not be sensitive to intracellular Ca^{2+} buffering or changes in extracellular Ca^{2+} and intracellular K^+—which is the case for the FCCP-induced current. Moreover, the H^+ equilibrium potential under our conditions is −30 mV and too positive with respect to the reversal potential of the current. Nevertheless, we cannot assume that the measured reversal potential is dependent solely on a single type of channel. Additional currents (mediated by H^+ channels, exchangers, or ionophores) could be activated by FCCP and render the measured reversal potential a sum of reversal potentials, which is merely dominated by the Ca^{2+}-activated cation channel we have characterized (see following text). FCCP could lower intracellular pH by drawing H^+ out of acidic stores (Park et al. 2002; Werth and Thayer 1994). Yet a drop of merely half a pH unit would render the H^+ equilibrium potential too negative at −60 mV. Acidification could activate pH-sensitive cation channels, but unlike the FCCP-induced current, such channels are blocked by ruthenium red (Garcia-Hirschfeld et al. 1995; Zeilhofer et al. 1996). Also the lack of an effect of bafilomycin A, which itself could acidify the cytosol, points away from H^+ as a gating factor. Finally, FCCP and related protonophores fail to depolarize or produce a current in hamster kidney, RBL-1, and chromaffin cells (Bashford et al. 1985; Giovannucci et al. 1999; Glitsch et al. 2002; Hernandez-Guijo et al. 2001) as well as crayfish motor and hippocampal neurons (Partridge and Valenzuela 1999; Tang and Zucker 1997). If FCCP generally caused depolarization, this would manifest in all cell types.

The FCCP-induced current is mainly voltage independent, accompanied by an increase in conductance, and presents a reversal potential of −40 mV, indicative of opening a nonselective cation channel. A reversal potential between −40 and +20 mV is characteristic of a varying degree of cation selectivity and no clear preference (Colquhoun et al. 1981; Kass et al. 1978; Partridge and Swandulla 1987; Partridge et al. 1994). Without external Ca^{2+}, the FCCP-induced current is diminished, and the reversal shifts to the left, implying Ca^{2+} passes. Similarly, dialysis with a low K^+ intracellular saline, such that the K^+ equilibrium potential changes from around −100 mV to close to −50 mV, shifts the reversal to approximately −20 mV. However, Cl^- does not seem to play a role given that the current is unaffected by moving the Cl^- equilibrium potential from −50 mV to near 0 mV after dialyzing with high Cl^- intracellular saline.

Because a rise in intracellular Ca^{2+} appears to elicit the current, one or more bag cell neuron Ca^{2+}-activated channels may be responsible. The voltage-dependent cation channel characterized by Wilson et al. (1996) and Geiger et al. (2009) is an unlikely candidate given that it reverses well above 0 mV, although it may contribute to the depolarization through secondary activation. A second remote prospect is the voltage-independent cation channel that reverses around −15 mV and is opened by flufenamic acid-mediated Ca^{2+} release (Gardam et al. 2008). The most likely possibility is the voltage-independent cation channel reported by Hung and Magoski (2007) that is triggered by Ca^{2+} influx, reverses near −40 mV, and is not blocked by Ni^{2+} or SKF-96365 (Tam et al. 2009). In the present study, a version of this current was evoked by a train of depolarizing stimuli and shown to be insensitive to NEM.

Where the present study suggests a link between mitochondrial Ca^{2+} and channel activation, other reports point to metabolic or Ca^{2+} buffering roles for mitochondria in regulating plasma membrane channels. For example, FCCP generates an outward current in hippocampal and locus ceruleus neurons (Hyllienmark and Brismar 1996; Murai et al. 1997; Nowicky and Duchen 1998). Those studies suggest that a reduction in ATP both opens K_{ATP} channels and, through a lessening of the Ca^{2+} ATPase, leads to a leak of endoplasmic reticulum Ca^{2+} that in turn gates Ca^{2+}-activated K^+ channels. Furthermore, store-operated channels in Chinese hamster ovary and Jurkat T-cells, as well as IP_3 receptors in HeLa cells, are inhibited by mitochondrial depolarization but not by transition pore block

(Cho et al. 1997; Collins et al. 2000). Thus, work using other preparations does not point to mitochondrial Ca^{2+} per se as a trigger for channel gating. Our data on bag cell neurons fail to establish that simply inhibiting mitochondrial ATP production will open membrane channels; rather, mitochondrial Ca^{2+} appears to be vital.

In a number of neurons, endoplasmic reticulum Ca^{2+} either evokes or potentiates voltage-independent cation channels. Ca^{2+}-induced Ca^{2+} release enhances depolarizing afterpotentials in supraoptic and hippocampal neurons (Li and Hatton 1997; Partridge and Valenzula 1999). Metabotropic or CPA-stimulated Ca^{2+} release impacts cation channels in dorsal root ganglion and supraoptic neurons (Crawford et al. 1997; Li et al. 1999) and turns on certain transient receptor potential channels in expression systems (Launay et al. 2002; Liu and Liman 2003; Prawitt et al. 2003; Strubing et al. 2001; Zitt et al. 1997). However, gating of such currents by mitochondrial Ca^{2+} has not been reported until now. Cultured bag cell neurons are both quite resistive and present a sizeable membrane surface area, resulting in a large membrane time constant. Thus once the cation current has depolarized the neuron, it may be lengthened in part by the time constant slowing recovery of the membrane potential. Because bag cell neurons release mitochondrial Ca^{2+} during prolonged action potential firing (Fisher et al. 1994; Geiger and Magoski 2008), the cation channel could contribute to the depolarization necessary for the afterdischarge.

Why does endoplasmic reticulum Ca^{2+} fail to open channels? Potentially, the reduced magnitude, rate, or duration of the Ca^{2+} rise elicited by CPA, compared with FCCP, limits the ability of endoplasmic reticulum Ca^{2+} to trigger current. That stated, the persistence of the FCCP response at low doses or in the face of a reduced Ca^{2+} response under NEM suggests that the size of the Ca^{2+} signal is less of a factor, i.e., a small amount of mitochondrial Ca^{2+} still evokes a current. Differential distribution may give mitochondrial Ca^{2+} preferential physical access to membrane channels. For example, in oligodendrocytes, mitochondria are localized to areas of Ca^{2+} signal amplification during wave propagation (Simpson and Russell 1996). Endoplasmic reticulum is sometimes more associated with the nucleus, while mitochondria are evenly distributed (Palade 1955; Verkhratsky 2005). Accordingly, dye staining of bag cell neurons shows mitochondria are present throughout the soma and neurites (White and Kaczmarek 1997). Alternatively, the channel could be gated by an intermediate, yet mobile Ca^{2+} sensor, such as calmodulin. Both Wood et al. (1980) and Pardue et al. (1981) provide evidence that calmodulin tightly associates with mitochondria. Our laboratory has established that both calmodulin and various enzymes can closely associate with channels in bag cell neurons (Gardam and Magoski 2009; Lupinsky and Magoski 2006; Magoski 2004; Magoski and Kaczmarek 2005). If the Ca^{2+} sensor favors association with the mitochondria, as opposed to the endoplasmic reticulum, then mitochondrial Ca^{2+} could be privileged for channel activation. In fact, this may be key to why simply increasing Ca^{2+} with CPA or bafilomycin does not have an effect. Finally, along with opening the cation channel, a secondary Ca^{2+}-dependent process could synergize with mechanisms already discussed (lengthy time constant, voltage-dependent channels) to extend or further the depolarization.

To summarize, Ca^{2+} from mitochondria opens a cation channel that profoundly impacts neuronal activity. This regulation appears unique in so much that it is not recapitulated by endoplasmic reticulum Ca^{2+}. Given the role of mitochondrial permeability in apoptosis and excitotoxicity (Campanella et al. 2004; Galluzzi et al. 2009), gating of a depolarizing current by this Ca^{2+} source also has implications for pathophysiology.

ACKNOWLEDGMENTS

The authors thank S. L. Smith for technical assistance, N. M. Magoski for evaluation of previous drafts of the manuscript, and Dr. C. A. Ward for advice as well the generous gift of xanthine and xanthine oxidase. C. M. Hickey held an Ontario Graduate Scholarship in Science and Technology and N. S. Magoski holds a Canadian Institutes of Health Research New Investigator Award.

GRANTS

This work was supported by a Canadian Institute of Health Research operating grant to N. S. Magoski.

REFERENCES

Acosta-Urquidi J, Dudek FE. Soma spike of neuroendocrine bag cells of *Aplysia californica*. *J Neurobiol* 12: 367–378, 1981.

Albert AP, Large WA. Synergism between inositol phosphates and diacylglycerol on native TRPC6-like channels in rabbit portal vein myocytes. *J Physiol* 552: 789–795, 2003.

Bardo S, Cavazzini MG, Emptage N. The role of the endoplasmic reticulum Ca^{2+} store in the plasticity of central neurons. *Trends Pharmacol Sci* 27: 78–84, 2006.

Bashford CL, Alder GM, Gray MA, Micklem KJ, Taylor CC, Turek P, Pasternak CA. Oxonol dyes as monitors of membrane potential: the effect of viruses and toxins on the plasma membrane potential of animal cells in monolayer culture and in suspension. *J Cell Physiol* 123: 326–336, 1985.

Billups B, Forsythe ID. Presynaptic mitochondrial calcium sequestration influences transmission at mammalian central synapses. *J Neurosci* 22: 5840–5847, 2002.

Bowman EJ, Siebers A, Altendorf K. Bafilomycins: a class of inhibitors of membrane atpases from microorganisms, animal cells, and plant cells. *Proc Natl Acad Sci USA* 85: 7972–7976, 1988.

Brinley FJ Jr, Tiffert JT, Mullins LJ, Scarpa A. Kinetic measurement of Ca^{2+} transport by mitochondria in situ. *FEBS Lett* 82: 197–200, 1977.

Cabello OA, Schilling WP. Vectorial Ca^{2+} flux from the extracellular space to the endoplasmic reticulum via a restricted cytoplasmic compartment regulates inositol 1,4,5-triphosphate-stimulated Ca^{2+} release from internal stores in vascular enothelial cells. *Biochem J* 295: 357–366, 1993.

Campanella M, Pinton P, Rizzuto R. Mitochondrial Ca^{2+} homeostasis in health and disease. *Biol Res* 37: 653–60, 2004.

Chesnoy-Marchais D. Kinetic properties and selectivity of calcium-permeable single channels in *Aplysia* neurons. *J Physiol* 367: 457–488, 1985.

Cho JH, Balasubramanyam M, Chernaya G, Gardner JP, Aviv A, Reeves JP, Dargis PG, Christian EP. Oligomycin inhibits store-operated channels by a mechanism independent of its effects on mitochondrial ATP. *Biochem J* 324: 971–980, 1997.

Christensen KA, Myers JT, Swanson JA. pH-dependent regulation of lysosomal calcium in macrophages. *J Cell Sci* 115: 599–607, 2002.

Colegrove SL, Albrecht MA, Friel DD. Dissection of mitochondrial Ca^{2+} uptake and release fluxes in situ after depolarization evoked $[Ca^{2+}]_i$ elevations in sympathetic neurons. *J Gen Physiol* 115: 351–369, 2000.

Collins TJ, Lipp P, Berridge MJ, Li W, Bootman MD. Inositol 1,4,5-trisphosphate-induced Ca^{2+} release is inhibited by mitochondrial depolarization. *Biochem J* 347: 593–600, 2000.

Colquhoun D, Neher E, Reuter H, Stevens CF. Inward current channels activated by intracellular Ca in cultured cardiac cells. *Nature* 294: 752–754, 1981.

Conn PJ, Kaczmarek LK. The bag cell neurons of Aplysia. *Mol Neurobiol* 3: 237–273, 1989.

Costantini P, Chernyak BV, Petronilli C, Bernardi P. Modulation of the mitochondrial permeability transition pore by pyridine nucleotides and dithiol oxidation at two separate sites. *J Biol Chem* 271: 6746–6751, 1996.

Crawford JH, Wootton JF, Seabrook GR, Scott RH. Activation of Ca^{2+}-dependent currents in dorsal root ganglion neurons by metabotropic glutamate receptors and cyclic ADP-ribose precursors. *J Neurophysiol* 77: 2573–2584, 1997.

Emptage NJ, Reid CA, Fine A. Calcium stores in hippocampal synaptic boutons mediate short-term plasticity, store-operated Ca^{2+} entry and spontaneous transmitter release. *Neuron* 29: 197–208, 2001.

Fisher TE, Levy S, Kaczmarek LK. Transient changes in intracellular calcium associated with a prolonged increase in excitability in neurons of Aplysia californica. *J Neurophysiol* 71: 1254–1257, 1994.

Fluharty AL, Sanadi DR. On the mechanism of oxidative phosphorylation. VI. Localization of the dithiol in oxidative phosphorylation with respect to the oligomycin inhibition site. *Biochemistry* 2: 519–22, 1963.

Friel DD, Chiel HJ. Calcium dynamics: analyzing the Ca^{2+} regulatory network in intact cells. *Trends Neurosci* 31: 8–19, 2008.

Friel DD, Tsien RW. An FCCP-Sensitive Ca^{2+} Store in bullfrog sympathetic neurons and its participation in stimulus-evoked changes in $[Ca^{2+}]_i$. *J Neurosci* 14: 4007–4024, 1994.

Fulceri R, Bellomo G, Mirabelli F, Gamberucci A, Benedetti A. Measurement of mitochondrial and non-mitochondrial Ca^{2+} in isolated intact hepatocytes: a critical re-evaluation of the use of mitochondrial inhibitors. *Cell Calcium* 12: 431–439, 1991.

Galluzzi L, Blomgren K, Kroemer G. Mitochondrial membrane permeabilization in neuronal injury. *Nat Rev Neurosci* 10: 481–494, 2009.

García-Hirschfeld J, López-Briones LG, Belmonte C, Valdeolmillos M. Intracellular free calcium responses to protons and capsaicin in cultured trigeminal neurons. *Neuroscience* 67: 235–243, 1995.

Gardam KE, Geiger JE, Hickey CM, Hung AY, Magoski NS. Flufenamic acid affects multiple currents and causes intracellular Ca^{2+} release in *Aplysia* bag cell neurons. *J Neurophysiol* 100: 38–49, 2008.

Gardam KE, Magoski NS. Regulation of cation channel voltage- and Ca^{2+}-dependence by multiple modulators. *J Neurophysiol* 102: 259–271, 2009.

Geiger JE, Hickey CM, Magoski NS. Ca^{2+} entry through a non-selective cation channel in *Aplysia* bag cell neurons. *Neuroscience* 162: 1023–1038, 2009.

Geiger JE, Magoski NS. Ca^{2+}-induced Ca^{2+}-release in *Aplysia* bag cell neurons requires interaction between mitochondrial and endoplasmic reticulum stores. *J Neurophysiol* 100: 24–37, 2008.

Giovannucci DR, Hlubek MD, Stuenkel EL. Mitochondria regulate the Ca^{2+}-exocytosis relationship of bovine adrenal chromaffin cells. *J Neurosci* 19: 9261–9270, 1999.

Glitsch MD, Bakowski D, Parekh AB. Store-operated Ca^{2+} entry depends on mitochondrial Ca^{2+} uptake. *EMBO J* 21: 6744–6754, 2002.

Goncalves PP, Meireles SM, Neves P, Vale MG. Synaptic vesicle Ca^{2+}/H^{+} antiport: dependence on the proton electrochemical gradient. *Mol Brain Res* 71: 178–84, 1999.

Greer PL, Greenberg ME. From synapse to nucleus: calcium-dependent gene transcription in the control of synapse development and function. *Neuron* 59: 846–860, 2008.

Hernández-Guijo JM, Maneu-Flores VE, Ruiz-NuZo A, Villarroya M, García AG, Gandía L. Calcium-dependent inhibition of L, N, and P/Q Ca^{2+} channels in chromaffin cells: role of mitochondria. *J Neurosci* 21: 2553–2560, 2001.

Heytler PG, Prichard WW. A new class of uncoupling agents - carbonyl cyanide phenylrydrazones. *Biochem Biophys Res Comm* 7: 272–275, 1962.

Hickey CM. *Ca^{2+} Influx and Release Controls Neuroendocrine Cell Secretion and Excitability* (MSc thesis). Kingston, Ontario, Canada: Queen's University, 2009.

Hung AY, Magoski NS. Activity-dependent initiation of a prolonged depolarization in *Aplysia* bag cell neurons: role for a cation channel. *J Neurophysiol* 97: 2465–2479, 2007.

Hunter DR, Haworth RA. The Ca^{2+}-induced membrane transition in mitochondria. I. The protective mechanisms. *Arch Biochem Biophys* 195: 453–459, 1979.

Hyllienmark L, Brismar T. Effect of metabolic inhibition on K^{+} channels in pyramidal cells of the hippocampal CA1 region in rat brain slices. *J Physiol* 496: 155–164, 1996.

Jonas EA, Knox RJ, Smith TCM, Wayne NL, Connor JA, Kaczmarek LK. Regulation by insulin of a unique neuronal Ca^{2+} pool and neuropeptide secretion. *Nature* 385: 343–346, 1997.

Kachoei BA, Knox RJ, Uthuza D, Levy S, Kaczmarek LK, Magoski NS. A store-operated Ca^{2+} influx pathway in the bag cell neurons of Aplysia. *J Neurophysiol* 96: 2688–2698, 2006.

Kass RS, Lederer WJ, Tsien RW, Weingart R. Role of calcium ions in transient inward currents and aftercontractions induced by strophanthidin in cardiac Purkinje fibers. *J Physiol* 281: 187–208, 1978.

Khoutorsky A, Spira ME. Calpain inhibitors alter the excitable membrane properties of cultured *Aplysia* neurons. *J Neurophysiol* 100: 2784–2793, 2008.

Kirichok Y, Krapivinsky G, Clapham DE. The mitochondrial calcium uniporter is a highly selective ion channel. *Nature* 427: 360–364, 2004.

Kupfermann I. Stimulation of egg laying: possible neuroendocrine function of bag cells of abdominal ganglion of *Aplysia californica. Nature* 216: 814–815, 1967.

Land SC, Porterfield DM, Sanger RH, Smith PJ. The self-referencing oxygen-selective microelectrode: detection of transmembrane oxygen flux from single cells. *J Exp Biol* 202: 211–218, 1999.

Lardy HA, Johnson D, McMurray WC. Antibiotics as tools for metabolic studies. I. A survey of toxic antibiotics in respiratory, phosphorylative and glycolytic systems. *Arch Biochem Biophys* 78: 587–597, 1958.

Launay P, Fleig A, Perraud AL, Schareberg AM, Penner R, Kinet JP. TRPM4 is a Ca^{2+}-activated nonselective cation channel mediating cell membrane depolarization. *Cell* 109: 397–407, 2002.

Levitan IB. It is calmodulin afer all! Mediator of the calcium modulation of multiple ion channels. *Neuron* 22: 645–648, 1999.

Li Z, Hatton GI. Ca^{2+} release from internal stores: role in generating depolarizing after-potentials in rat supraoptic neurons. *J Physiol* 498: 339–350, 1997.

Li Z, Miyata S, Hatton GI. Inositol 1,4,5-triphosphate-sensitive Ca^{2+} stores in rat supraoptic neurons: involvement in histamine-induced enhancement of depolarizing afterpotentials. *Neuroscience* 93: 667–674, 1999.

Link EM, Riley PA. Role of hydrogen peroxide in the cytotoxicity of the xanthine/xanthine oxidase system. *Biochem J* 249: 391–399, 1988.

Liu D, Liman ER. Intracellular Ca^{2+} and the phospholipids PIP_2 regulate the taste transduction ion channel TRPM5. *Proc Nat Acad Sci USA* 100: 15160–15165, 2003.

Lupinsky DA, Magoski NS. Ca^{2+}-dependent regulation of a non-selective cation channel from *Aplysia* bag cell neurons. *J Physiol* 575: 491–506, 2006.

Magoski NS. Regulation of an *Aplysia* bag cell neuron cation channel by closely associated protein kinase A and a protein phosphatase. *J Neurosci* 24: 6833–6841, 2004.

Magoski NS, Kaczmarek LK. Association/dissociation of a channel-kinase complex underlies state-dependent modulation. *J Neurosci* 25: 8037–8047, 2005.

Magoski NS, Knox RJ, Kaczmarek LK. Activation of a Ca^{2+}-permeable cation channel produces a prolonged attenuation of intracellular Ca^{2+} release in *Aplysia* bag cell neurons. *J Physiol* 522: 271–283, 2000.

Mani SK, Shiraishi H, Balasubramanian S, Yamane K, Chellaiah M, Cooper G, Banik N, Zile MR, Kuppuswamy D. In vivo administration of calpeptin attenuates calpain activation and cardiomyocyte loss in pressure-overloaded feline myocardium.*Am J Physiol Heart Circ Physiol* 295: H314–H326, 2008.

Matlib MA, Zhou Z, Ahmed KS, Choi KM, Krause-Baueri J, Phillips R, Altschuld R, Katsube Y, Sperelakis N, Bers DM. Oxygen-bridged dinuclear ruthenium amine complex specifically inhibits Ca^{2+} uptake into mitochondria in vitro and in situ in single cardiac myocytes. *J Biol Chem* 273: 10223–10231, 1998.

Mercer NA, McKelvey JR, Fioravanti CF. *Hymenolepis diminuta*: catalysis of transmembrane proton translocation by mitochondrial NADPH–>NAD transhydrogenase. *Exp Parasitol* 91: 52–58, 1999.

Moore CL. Specific inhibition of mitochondrial Ca^{++} transport by ruthenium red. *Biochem Biophys Res Comm* 42: 298–305, 1971.

Murai Y, Ishibashi H, Koyama S, Akaike N. Ca^{2+}-activated K^{+} currents in rat locus coeruleus neurons induced by experimental ischemia, anoxia, and hypoglycemia. *J Neurophysiol* 78: 2674–2681, 1997.

Naraghi M. T-jump study of calcium binding kinetics of calcium chelators. *Cell Calcium* 22: 255–268, 1997.

Neher E, Sakaba T. Multiple roles of calcium ions in the regulation of neurotransmitter release. *Neuron* 59: 861–872, 2008.

Nilius B. From TRPs to SOCs, CCEs, and CRACs: consensus and controversies. *Cell Calcium* 33: 293–298, 2003.

Nowicky AV, Duchen MR. Changes in $[Ca^{2+}]_i$ and membrane currents during impaired mitochondrial metabolism in dissociated rat hippocampal neurons. *J Physiol* 507: 131–145, 1998.

Palade GE. Studies on the endoplasmic reticulum. II. Simple dispositions in cells in situ. *J Biophys Biochem Cytol* 25: 567–582, 1955.

Pardue RL, Kaetzel MA, Hahn SH, Brinkley BR, Dedman JR. The identification of calmodulin-binding sites on mitochondria in cultured 3T3 cells. *Cell* 23: 533–542, 1981.

Park K-S, Jo I, Pak YK, Bae, S-W, Rhim H, Suh S-H, Park SJ, Zhu MH, So I, Kim KW. FCCP depolarizes plasma membrane potential by activating proton and Na^+ currents in bovine aortic endothelial cells. *Pfluegers Eur J Physiol* 443: 344–352, 2002.

Partridge LD, Muller TH, Swandulla D. Calcium-activated non-selective channels in the nervous system. *Brain Res Rev* 19: 310–325, 1994.

Partridge LD, Swandulla D. Single Ca^{2+}-activated cation channels in bursting neurons of. *Helix. Pfluegers* 410: 627–631, 1987.

Partridge LD, Valenzuela CF. Ca^{2+} store-dependent potentiation of Ca^{2+}-activated non-selective cation channels in rat hippocampal neurons in vitro. *J Physiol* 521: 617–627, 1999.

Petronilli V, Costantini P, Scorrano L, Colonna R, Passamonti S, Bernardi P. The voltage sensor of the mitochondrial permeability transition pore is tuned by the oxidation-reduction state of vicinal thiols. Increase of the gating potential by oxidants and its reversal by reducing agents. *J Biol Chem* 269: 16638–16642, 1994.

Pinsker HM, Dudek FE. Bag cell control of egg laying in freely behaving *Aplysia. Science* 197: 490–493, 1977.

Prawitt D, Monteilh-Zoller MK, Brixel L, Spangenberg C, Zabel B, Fleig A, Penner R. TRPM5 is a transient Ca^{2+}-activated cation channel responding to rapid changes in $[Ca^{2+}]_i$. *Proc Nat Acad Sci USA* 100: 15166–15171, 2003.

Richter TA, Kolaj M, Renaud LP. Low voltage-activated Ca^{2+} channels are coupled to Ca^{2+}-induced Ca^{2+} release in rat thalamic midline neurons. *J Neurosci* 25: 8267–8271, 2005.

Seidler NW, Jona I, Vegh M, Martonosi A. Cyclopiazonic acid is a specific inhibitor of the Ca^{2+}-ATPase of sarcoplasmic reticulum. *J Biol Chem* 264: 17816–17823, 1989.

Simpson PB, Russell JT. Mitochondria support inositol 1,4,5-trisphosphate-mediated Ca^{2+} waves in cultured oligodendrocytes. *J Biol Chem* 271: 33493–33501, 1996.

Solovyova N, Veselovsky N, Toescu NC, Verkhratsky A. Ca^{2+} dynamics in the lumen of the endoplasmic reticulum in sensory neurons: direct visualization of Ca^{2+} -induced Ca^{2+} release triggered by physiological Ca^{2+} entry. *EMBO* 21: 622–630, 2002.

Spira ME, Oren R, Dormann A, Ilouz N, Lev S. Calcium, protease activation, and cytoskeleton remodeling underlie growth cone formation and neuronal regeneration *Cell Mol Neurobiol* 21: 591–604, 2001.

Strubing C, Krapivinsky G, Krapivinsky L, Clapham DE. TRPC1 and TRPC5 form a novel cation channel in mammalian brain. *Neuron* 29: 645–655, 2001.

Tam AKT, Geiger JE, Hung AY, Groten CJ, Magoski NS. Persistent Ca^{2+} current contributes to a prolonged depolarization in *Aplysia* bag cell neurons. *J Neurophysiol* 102: 3753–3765, 2009.

Tang Y-G, Zucker RS. Mitochondrial involvement in post-tetanic potentiation of synaptic transmission. *Neuron* 18: 483–491, 1997.

Thastrup O, Cullen PJ, Drobak BK, Hanley MR, Dawson AP. Thapsigargin, a tumor promoter, discharges intracellular Ca^{2+} stores by specific inhibition of the endoplasmic reticulum Ca^{2+}-ATPase. *Proc Natl Acad Sci USA* 87: 2466–2470, 1990.

Tatsumi H, Katayama Y. Brief increases in intracellular Ca^{2+} activate K^+ current and non-selective cation current in rat nucleus basalis neurons. *Neuroscience* 58: 553–561, 1994.

Tsujinaka T, Kajiwara Y, Kambayashi J, Sakon M, Higuchi N, Tanaka T, Mori T. Synthesis of a new cell penetrating calpain inhibitor (calpeptin). *Biochem Biophys Res Comm* 153: 1201–1208, 1988.

Verkhratsky A. Physiology and pathophysiology of the calcium store. *Physiol Rev* 85: 201–279, 2005.

Vorndran C, Minta A, Poenie M. New fluorescent calcium indicators designed for cytosolic retention or measuring calcium near membranes. *Biophys J* 69: 2112–2124, 1995.

Werth JL, Thayer SA. Mitochondria buffer physiological calcium loads in cultured rat dorsal root ganglion neurons. *J Neurosci* 14: 348–356, 1994.

White BH, Kaczmarek LK. Identification of a vesicular pool of calcium channels in the bag cell neurons of Aplysia californica. *J Neurosci* 17: 1582–1595, 1997.

Wilson GF, Richardson FC, Fisher TE, Olivera BM, Kaczmarek LK. Identification and characterization of a Ca^{2+}-sensitive nonspecific cation channel underlying prolonged repetitive firing in *Aplysia* neurons. *J Neurosci* 16: 3661–3671, 1996.

Wingrove DE, Gunter TE. Kinetics of mitochondrial calcium transport. II. A kinetic description of the sodium-dependent calcium efflux mechanism of liver mitochondria and inhibition by ruthenium red and by tetraphenylphosphonium. *J Biol Chem* 261: 15166–15171, 1986.

Wood JG, Wallace RW, Whitaker IN, Cheung WY. Immunocytochemical localization of calmodulin and a heat-labile calmodulin-binding protein (CaM-BPS0) in basal ganglia of mouse brain. *J Cell Biol* 84: 66–76, 1980.

Zeilhofer HU, Swandulla D, Reeh PW, Kress M. Ca^{2+} permeability of the sustained proton-induced cation current in adult rat dorsal root ganglion neurons. *J Neurophysiol* 76: 2834–2840, 1996.

Zitt C, Zobel A, Obukhov AG, Harteneck C, Kalkbrenner F, Luckhoff A, Schultz G. Cloning and functional expression of a human Ca^{2+}-permeable cation channel activated by calcium store depeltion. *Neuron* 16: 1189–1196, 1997.

J Neurophysiol 103: 2934, 2010.
doi:10.1152/jn.z9k-0126-corr.2010.

Volume 103, March 2010

Hickey CM, Geiger JE, Groten CJ, Magoski NS. Mitochondrial Ca^{2+} Activates a Cation Current in *Aplysia* Bag Cell Neurons. *J Neurophysiol* 103: 1543–1556, 2010; doi:10.1152/jn.01121.2009; http://jn.physiology.org/cgi/content/full/103/3/1543.

During production an improved version of Fig. 9 (with respect to panel E) was not used. Here is the improved version.

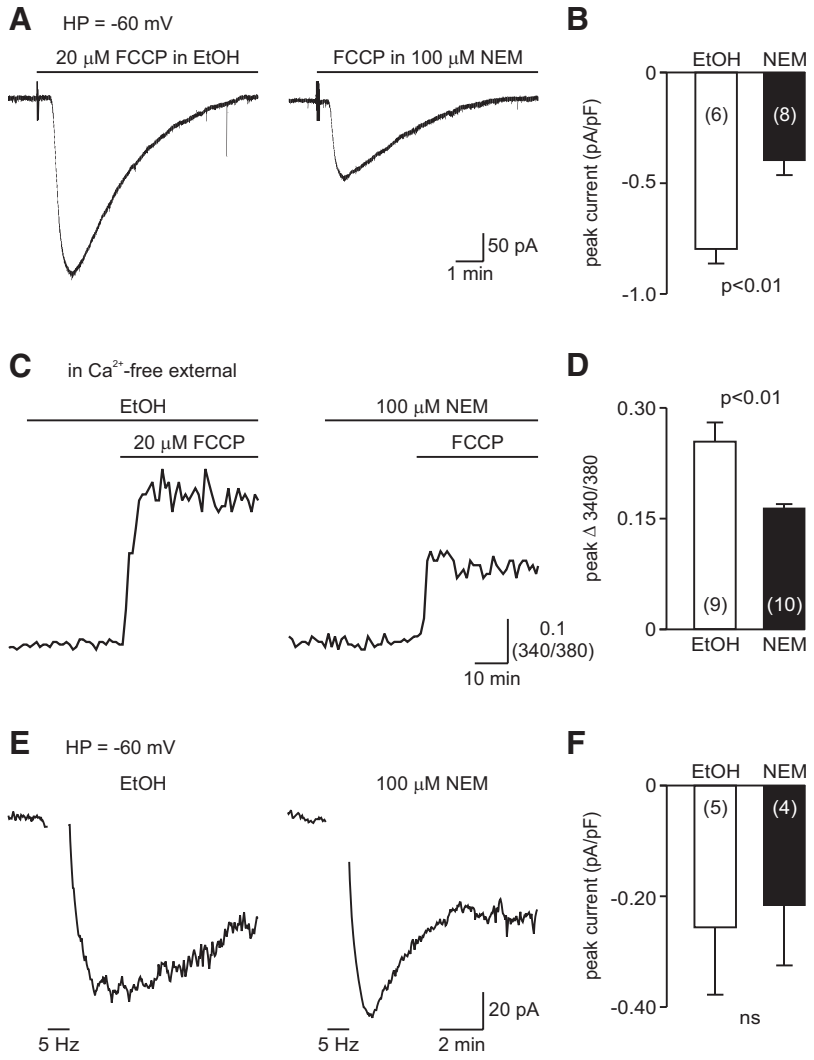

FIG. 9. An alkylating agent attenuates both the rise in intracellular Ca^{2+} and the current induced by FCCP. *A*: whole cell, voltage-clamp recordings at −60 mV, in separate neurons bathed in nASW, demonstrate a notable reduction in the amplitude of the FCCP-induced current following a 30-min pretreatment with 100 μM *N*-ethylmaleimide (NEM; *right*) but not the vehicle, ethanol (EtOH; *left*). *B*: summary data of mean peak current normalized to cell size indicate that the current evoked by 20 μM FCCP is significantly decreased subsequent to treatment with NEM versus ethanol (2-tailed unpaired *t*-test). *C*: monitoring intracellular Ca^{2+} with ratiometric imaging in Ca^{2+}-free external shows that 20 μM FCCP causes a prominent rise in cytosolic Ca^{2+} with ethanol (*left*); however, this effect is greatly diminished following a 30-min treatment with NEM (*right*). Note that application of ethanol or NEM alone does not alter intracellular Ca^{2+}. *D*: summary data show that the mean change in 340/380 evoked by FCCP is significantly less following NEM than after ethanol (2-tailed unpaired *t*-test; Welch corrected). *E*: current traces under voltage clamp at −60 mV from different neurons. Delivery (at bar) of a 5-Hz, 1-min train of 75-ms steps to +10 mV elicits an inward current. Compared with ethanol exposure (*left*), the magnitude of the train-evoked current subsequent to NEM (*right*) is similar. Differences in time-course following the peak are observed in both data sets and similar to our prior observations (see Hung and Magoski 2007 ↓). *F*: summary of average peak train-evoked current normalized to capacitance. This activity-dependent current is not significantly different when ethanol is compared with NEM (2-tailed unpaired *t*-test).